Mineralia Slovaca, Web ISSN 1338-3523, ISSN 0369-2086, https://doi.org/10.56623/ms.2025.57.2.2
57, 2 (2025), 111 – 144, © Authors 2025. CC BY 4.0

Heavy mineral analysis of the Upper Cretaceous to Lower Eocene synorogenic formations of the Pieniny Klippen Belt (Šariš Unit, eastern Slovakia): new data from the Jar-2 borehole (Jarmuta-Proč Fm.) and outcrops (Malinowa Fm.)

JOZEF MADZIN [1]* and DUŠAN PLAŠIENKA [2]

[1] Earth Science Institute, Slovak Academy of Sciences, Ďumbierska 1, 974 01 Banská Bystrica, Slovak Republic;
* corresponding author, jozef.madzin@savba.sk
[2] Comenius University, Faculty of Natural Sciences, Department of Geology and Palaeontology, Ilkovičova 6, 842 15 Bratislava, Slovak Republic; dusan.plasienka@uniba.sk

Abstract: The study presents new results of heavy mineral analyses including detrital garnet, tourmaline and Cr-rich spinel chemical compositions from the synorogenic Maastrichtian-Ypresian Jarmuta-Proč Fm. of the Šariš Unit of the Pieniny Klippen Belt, penetrated by the structural borehole Jar-2 in eastern Slovakia. For comparison, outcropped fine-grained sandstones of the hemipelagic Turonian-Campanian Malinowa Fm. of the Šariš Unit were analysed. The heavy mineral assemblages of both formations are dominated by garnet with variable amounts of apatite, rutile, tourmaline, zircon and subordinate Cr-rich spinel. Almandine-rich garnets with variable grossular, pyrope, and spessartine proportions prevail in both formations. Unusual complex-zoned X-vacant magnesio-foititic to foititic and schorlitic-dravitic tourmaline grains with fine intergrowth with quartz and abundant inclusions were revealed. Cr-rich spinels show chemistry typical for supra-subduction zone peridotites. The chemistry of the Cr-rich spinels and complex-zoned tourmalines supports their common provenance in the Meliata ophiolite-bearing complexes of the internal Western Carpathian zones. Decreasing-upward Cr-rich spinel contents in the Upper Cretaceous to Lower Eocene flysch deposits of the PKB is evident. A multiple recycling model in which flysch formations of the Klape Unit, situated in a false accretionary wedge position, formed the "proximal" source of the ophiolitic debris recycled to the younger clastic formations of the foreland basins is advocated.

Key words: Western Carpathians, Pieniny Klippen Belt, synorogenic deposits, garnet, tourmaline, Cr-rich spinel, geochemistry, provenance

Graphical abstract

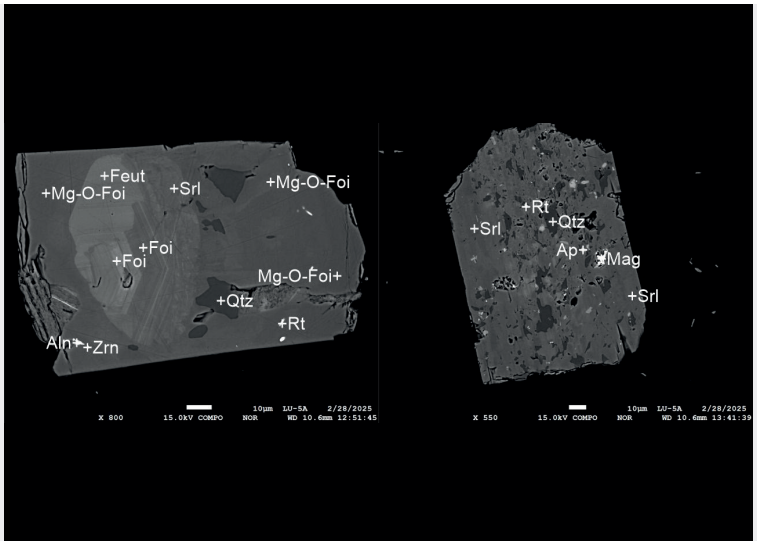

Highlights

- Unusual complex-zoned X-vacant magnesio-foititic to foititic and schorlitic-dravitic tourmaline grains with fine intergrowth with quartz and abundant inclusions revealed.
- Chemistry of the Cr-rich spinels and complex-zoned tourmalines supports their provenance in the Meliata ophiolite-bearing complexes of the internal Western Carpathian zones.
- Albian-Cenomanian flysch formations of the Klape Unit in a false accretionary wedge position shed ophiolitic debris to the Upper Cretaceous to Lower Eocene clastic formations of the foreland basins.

Introduction

The external and internal zones of the Western Carpathians are sharply separated by a more than 600 km long but exceptionally narrow zone with an unusually complicated structure, known as the Pieniny Klippen Belt (PKB). Its complex polyphase structural deformation dominated by the Paleocene to Eocene nappe thrusting resulted in the superposition and juxtaposition of numerous lithologically and palaeogeographically distinct tectonic units (e.g., Birkenmajer, 1977, 1986; Mišík, 1997; Jurewicz, 2005, 2018; Plašienka & Mikuš, 2010; Plašienka, 2012a). Subsequent wrench deformations obliterated original fold-and-thrust

structures resulting in the peculiar "klippen" structure (e.g., Ratschbacher et al., 1993; Kováč & Hók, 1996; Plašienka et al., 2020). Therefore, the PKB is often characterized as a block-in-matrix structure or mélange formed by isolated rigid blocks "klippens" composed of competent Middle Jurassic to Lower Cretaceous carbonates surrounded by a soft matrix of the "klippen cover" consisting of Lower Jurassic and Upper Cretaceous to Palaeogene shales, marls and flysch formations (e.g., Birkenmajer, 1977; Plašienka & Mikuš, 2010; Jurewicz, 2018; Plašienka, 2018). The main tectonic units of the PKB s.s., were derived from an independent palaeogeographic domain known as the Oravic domain or Oravicum (Maheľ, 1986). It is thought that the Oravic domain represents the continental crustal fragment in the Middle Penninic position (analogous to the Briançonnais microcontinent, Tomek, 1993) surrounded by North Penninic (Valais-Rhenodanubian-Magura) and South Penninic (Ligurian-Piemont-Vahic) oceanic domains as a continuation of the oceanic tract of the Alpine Tethys to the Carpathian realm (e.g., Schmid et al., 2008; Plašienka, 2012a). The suture-like structure of the PKB is related to the collision of the Oravic continental fragment with the frontal parts of the Central Western Carpathian block after the closure and subduction of the Vahic oceanic domain (Plašienka, 2012a; Plašienka et al., 2020). The sedimentary record of the contractional tectonic processes is preserved in the Upper Cretaceous to Lower Eocene synorogenic flysch or wildflysch deposits including huge olistostromatic bodies and bodies of polymict "exotic" conglomerates (Mišík & Marschalko, 1988; Plašienka & Mikuš, 2010; Plašienka, 2012a; Plašienka et al., 2012; Golonka et al., 2015). In addition to the diverse pebble material of the conglomerates, the heavy mineral associations of psammitic deposits of the synorogenic formations also provide valuable information about provenance and composition of completely eroded or subducted source terrains (Salata, 2004; Aubrecht et al., 2009, 2021; Bellová et al., 2018; Bónová et al., 2018; Madzin et al., 2019). This study presents new results of heavy mineral analyses including detrital garnet, tourmaline and Cr-rich spinel chemical compositions from the synorogenic Maastrichtian-Ypresian Jarmuta-Proč Fm. of the Šariš Unit of the Pieniny Klippen Belt, penetrated by the structural borehole Jar-2 in eastern Slovakia. For comparison and revealing potential difference in composition and abundance of heavy mineral associations, outcropped fine-grained sandstones of the hemipelagic Turonian-Campanian Malinowa Fm. of the Šariš Unit were analysed as well.

Geological settings

The eastern branch of the PKB in eastern Slovakia forms almost straight NW-SE trending 3–5 km narrow zone, which is distinctly fault-bounded against the Paleogene flysch complexes of the Krynica Unit of the Magura nappe system toward the NE, as well as against the flysch deposits of the Central Carpathian Paleogene Basin (CCPB) towards the SW (Fig. 1) (Oszczypko et al., 2005; Jurewicz, 2018; Plašienka et al., 2020). The bounding faults are steeply NE-dipping up to vertical and show a complex kinematic history (e.g., Plašienka & Mikuš, 2010; Plašienka et al., 2013; Ludwiniak, 2018). The studied part of the PKB is dominantly composed of the Oravic units with relatively well-preserved original nappe edifice (Jurewicz, 1997, 2005, 2018; Plašienka & Mikuš, 2010; Plašienka, 2012b; Plašienka et al., 2020). In places, the original nappe structure was strongly modified by superimposed transpressional and transtensional deformations (e.g., Ratschbacher et al., 1993; Nemčok & Nemčok, 1994; Plašienka, 2012b; Plašienka et al., 2020). The completely detached Jurassic to Lower Eocene Oravic sedimentary successions have been assigned to the three main superposed and/or juxtaposed tectonic units (Figs. 1, 2) (Plašienka & Mikuš, 2010; Plašienka et al., 2012). These are from bottom to top and from the external to internal position the Šariš Unit and the Subpieniny and Pieniny thrust sheets. All three units are characterized by a thickening and coarsening upward clastic sedimentary successions (Fig. 2), manifesting the basin tectonic inversion and contractional tectonic regime due to the closure of the South Penninic Vahic Ocean and ensuing collision of the Oravic ribbon continent with the Central Western Carpathian block during the latest Cretaceous and Paleogene (Jurewicz, 2005; Plašienka, 2012a; Plašienka et al., 2020). In the topmost Pieniny thrust sheet, the youngest sediments are distal turbidites of the Turonian Snežnica Fm., passing to the thick-bedded sandstones with huge exotics-bearing conglomerates of the Coniacian-Santonian Sromowce Fm. (Starek et al., 2010; Plašienka, 2012a). The sedimentary succession of the Subpieniny thrust sheet is terminated by calcareous turbidites of the Maastrichtian-Danian Jarmuta Fm., with olistostromatic bodies known as the Gregorianka Breccia (Nemčok et al., 1989; redefined by Plašienka & Mikuš, 2010). The Jarmuta Fm. often occurs in an overturned position or is tectonically reduced and missing. In that case, the sedimentary succession of the Subpieniny nappe is terminated by variegated calcareous hemipelagites, with thin beds of fine- to medium-grained sandstones of the Jaworki Fm. (Birkenmajer, 1977, equivalent to the Púchov marls). The Šariš sedimentary succession is terminated by deepwater, poorly or completely non-calcareous, variegated hemipelagites with thin beds of siltstones to fine-grained sandstones of the Turonian-Campanian Malinowa Fm. (Birkenmajer, 1977). The Malinowa Fm. passes to thick clastic deposits of the Maastrichtian-Ypresian Jarmuta-Proč Fm. The Jarmuta-Proč Fm. involves deep-water turbidites with bodies of mass-flow deposits (Milpoš Breccia) (Plašienka & Mikuš, 2010), that consist of variegated

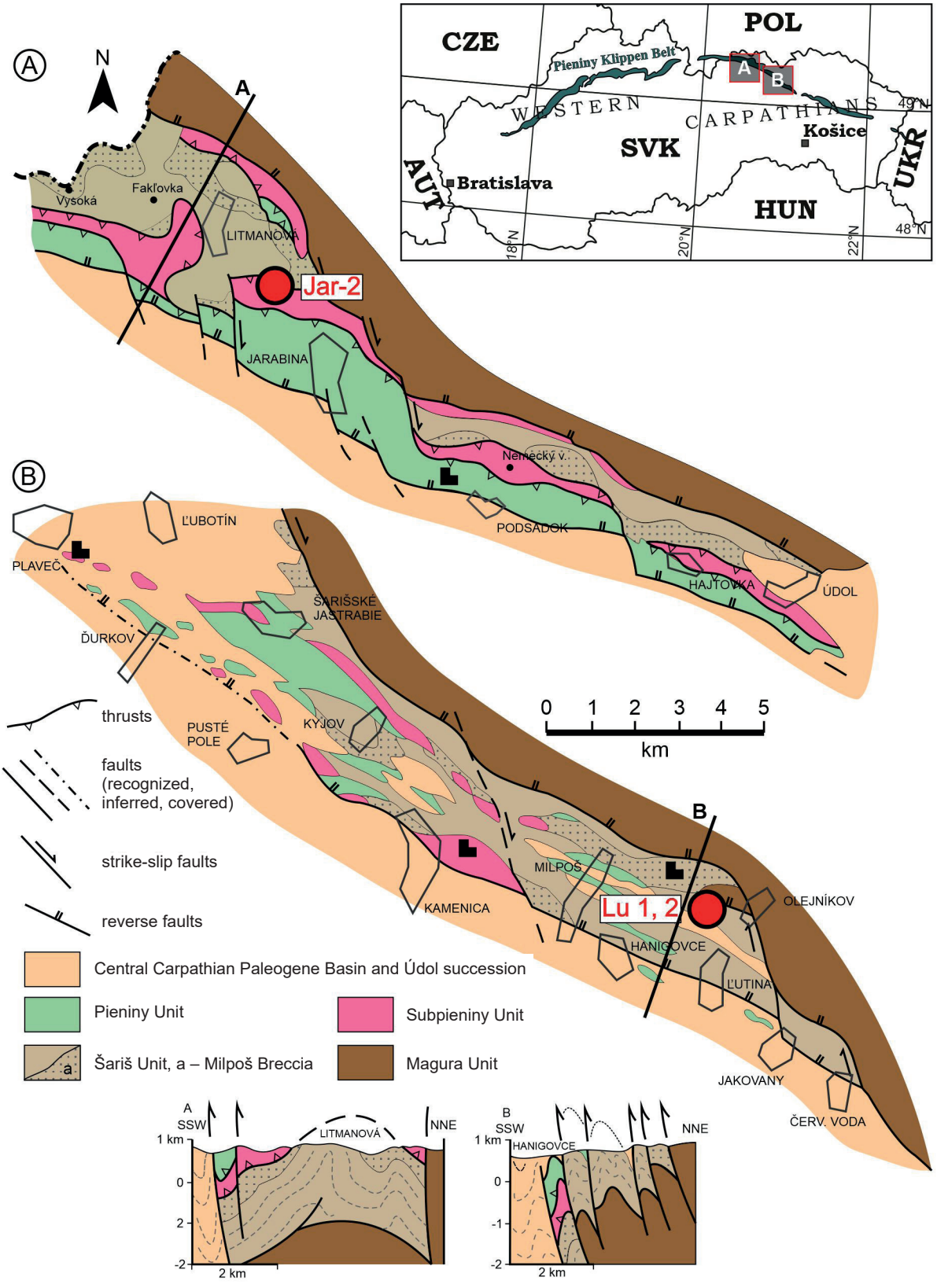

Fig. 1. Schematic tectonic maps of the eastern sector of the PKB between Litmanová and Červená Voda villages in eastern Slovakia with marked positions of the structural borehole Jar-2 and the studied outcrop near the village of Ľutina (modified according to Plašienka & Mikuš, 2010)

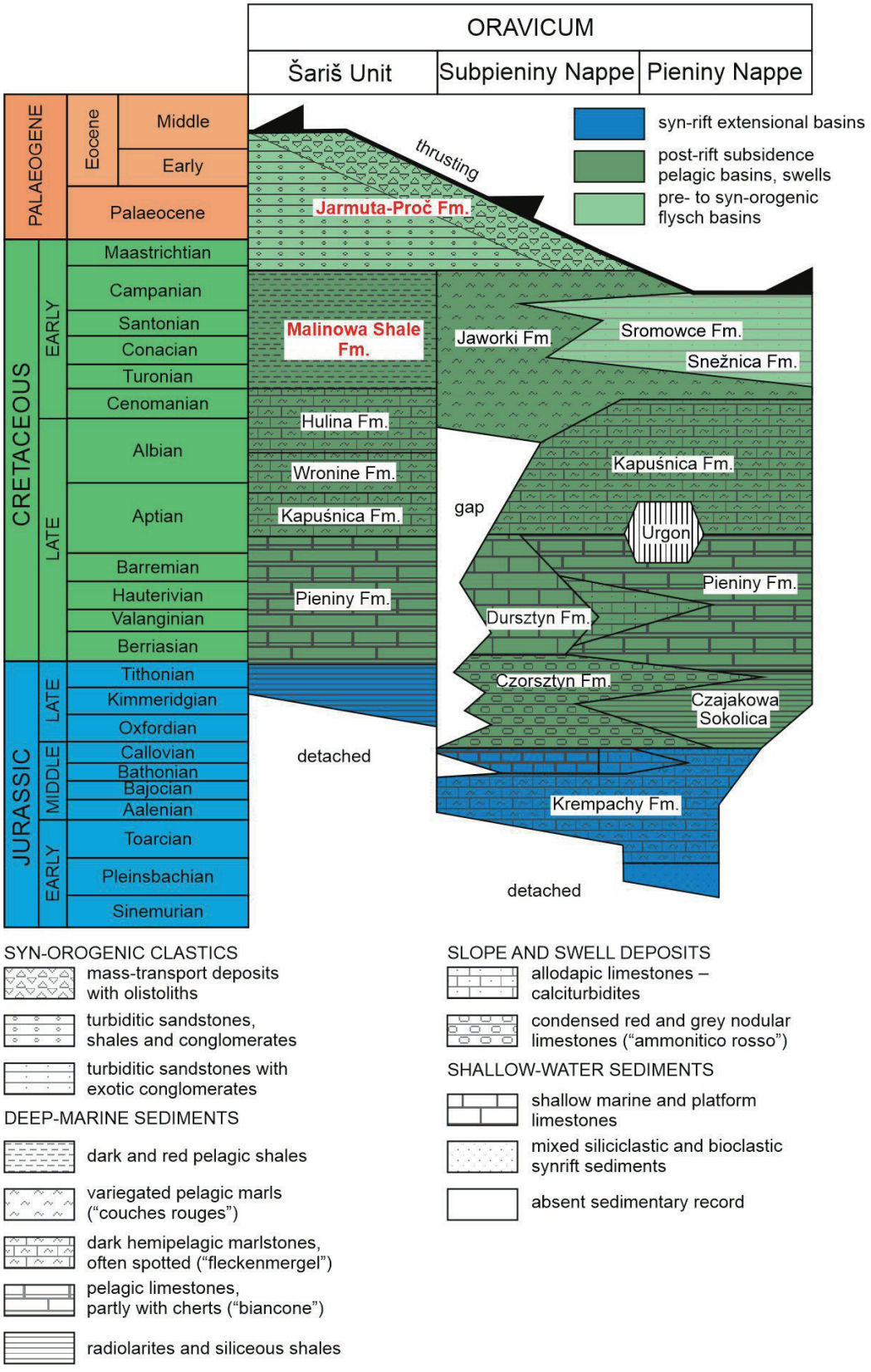

Fig. 2. Simplified lithostratigraphic column of the principal Oravic units of the Pieniny Klippen Belt (according to Plašienka, 2012a)

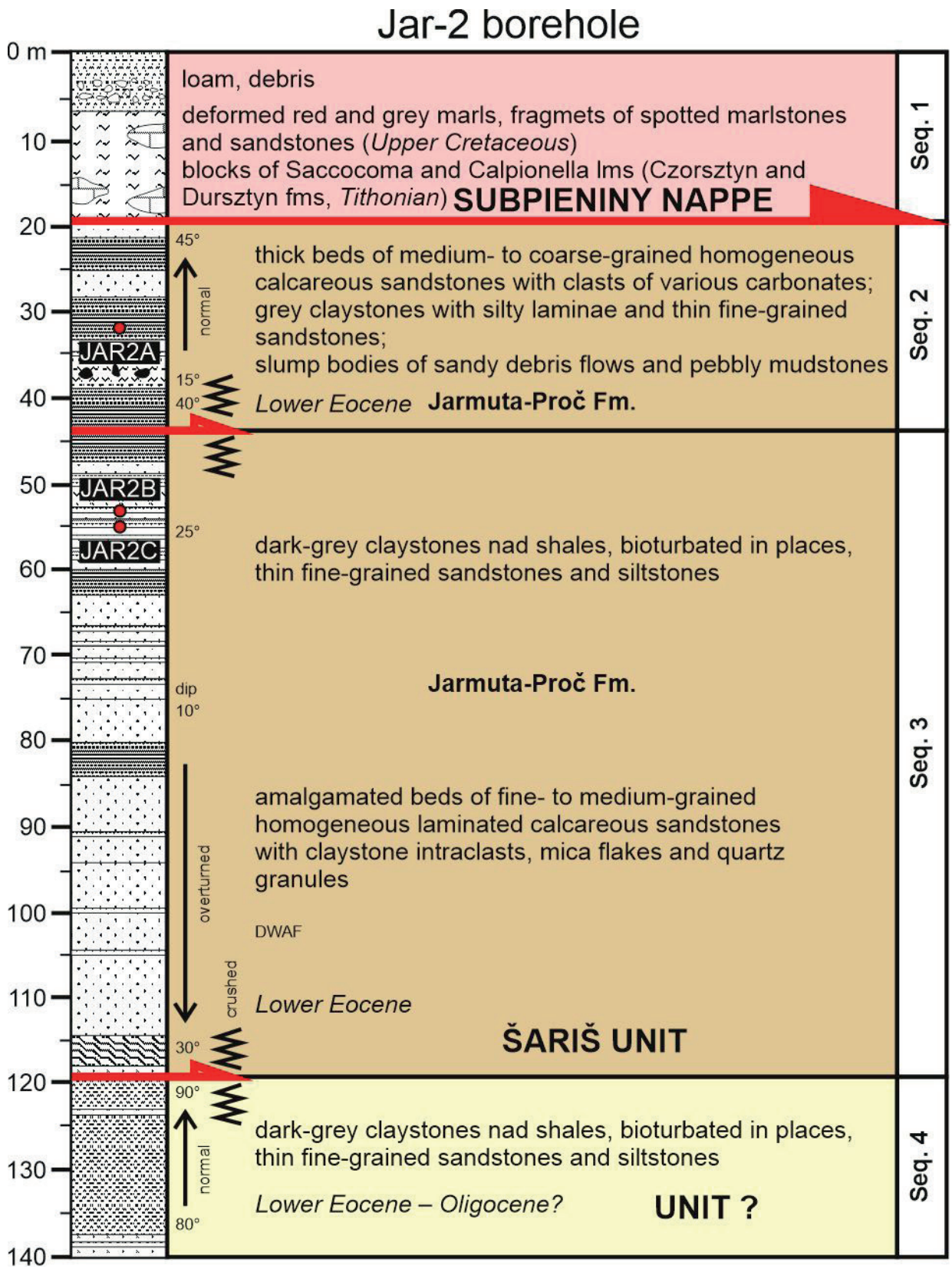

Fig. 3. Lithostratigraphic profile of the Jar-2 borehole, with the position of the samples taken for the heavy mineral analysis (modified after Plašienka et al., 2012)

clastic material derived dominantly from destroyed fronts of the advanced nappe stack (the Subpieniny and Pieniny thrust sheets).

Sampling and Methods

The studied material comes from a natural outcrop of thin-bedded fine-grained sandstones of the hemipelagic Turonian-Campanian Malinowa Fm. (Fig. 1, Tab. 1) and from thin-bedded siltstones to fine- to medium-grained sandstones of the core material of the structural borehole Jar-2 (Tab. 1, Figs. 1, 3), that penetrated a turbiditic sequence of the Maastrichtian-Ypresian Jarmuta-Proč Fm. of the Šariš Unit (Plašienka et al., 2012). Two boreholes Jar-1 and Jar-2 were drilled in winter 2009 near the village of Jarabina in the Pieniny sector of the PKB in eastern Slovakia (Figs. 1, 3). The Jar-2 borehole, with a core diameter of 4 cm, was continuously drilled to the final depth of 140 m. The borehole penetrated strongly deformed and overturned imbrications of the sedimentary successions of the Subpieniny nappe and several sequences of the Middle to Upper Cretaceous-Lower Eocene synorogenic sediments of the Šariš Unit (Fig. 3) (for more details, see Plašienka et al., 2012). The core material is stored at the Geological repository and borehole core collections of the State Geological Institute of Dionýz Štúr in Bratislava (Slovakia).

The sandstone samples for heavy mineral analyses (at least 1 kg each, due to availability of the core material) were cleaned, crushed and sieved under 250 μm. Then the 63–125 μm fraction was soaked in 10 % diluted cold acetic acid for at least 24 hours to dissolve carbonate content. After acidic treatment the fraction was cleaned in an ultrasonic bath and dried in an oven. Such prepared fraction was ready for the heavy liquid separation in LST heavy liquid (2.85 g/cm^3) using a separating funnel. Associations of heavy minerals were studied under a petrographic microscope Zeiss Axiom Scope A.1 and a stereomicroscope Olympus SZ-61 in both transmitted and reflected light. At least 200 grains were counted using the ribbon counting method (Galehouse, 1971) and shown as number percentages (Tab. 2).

Tab. 1

List of samples for heavy mineral analysis, with their geographic coordinates, lithostratigraphy and position in the borehole Jar-2

Sample	Locality	Lithostratigraphy	Lat	Lon	Note
Jar-2a	Jarabina, borehole Jar-2	Jarmuta-Proč Fm.	49.356583	20.638367	depth 33.0–33.4 m
Jar-2b	Jarabina, borehole Jar-2	Jarmuta-Proč Fm.	49.356583	20.638367	depth 52.5–52.7 m
Jar-2c	Jarabina, borehole Jar-2	Jarmuta-Proč Fm.	49.356583	20.638367	depth 55.3 m
Lu-5a	Ľutina	Malinowa Fm.	49.180861	21.042472	outcrop
Lu-5b	Ľutina	Malinowa Fm.	49.180861	21.042472	outcrop

Tab. 2

Frequencies of individual heavy minerals in the sandstones studied. Abbreviations of minerals (Whitney & Evans, 2010): Zrn – zircon, Tur – tourmaline, Rt – rutile, Grt – garnet, Spl – spinel, Ap – apatite, Cld – chloritoid, Ep – epidote, ZTR – zircon-tourmaline-rutile index, proportion of ultra-stable minerals (Hubert, 1962)

Sample	Zrn	Tur	Rt	Grt	Spl	Ap	Cld	Ep	ZTR
Jar-2A	1.0	26.9	8.5	36.3	0.5	24.9	1.0	1.0	36.3
Jar-2B	5.0	7.5	5.5	64.0	1.0	17.0	0.0	0.0	18.0
Jar-2C	5.4	5.9	7.9	69.0	1.0	10.8	0.0	0.0	19.2
Lu-5A	10.3	8.3	34.3	40.7	2.9	3.4	0.0	0.0	52.9
Lu-5B	12.5	2.5	22.5	59.0	3.0	0.5	0.0	0.0	37.5

Selected minerals including garnets, tourmalines and Cr-rich spinels were hand-picked, placed in an epoxy resin, polished and carbon coated for microprobe analyses. Chemical compositions of the selected minerals were analysed using a JEOL JXA-8530FE microprobe (Earth Science Institute of the Slovak Academy of Sciences, Banská Bystrica, Slovakia) under the following conditions: accelerating voltage 15 kV, sample current 20 nA, probe diameter 2–5 μm, counting time 10 s – peak and 5 s for background, ZAF correction. The standards used, including lines and detection limits (in ppm) were: Ca (Kα, 19–21) – diopside, Mn (Kα, 49–62) – rhodonite, Si (Kα, 45–50) – quartz, Mg (Kα, 35–37) – olivine, F (Kα, 112–294) – fluorite, Na (Kα, 31–36) – jadeite, Al (Kα, 38–40) – kyanite, K (Kα, 29–38) – orthoclase, Fe (Kα, 43–57) – hematite, Ti (Kα, 35–38) – rutile, Cr – (Kα, 71–130) – Cr_2O_3, Cl (Kα, 27–34) – tugtupite. The analyses of detrital garnets were normalized to 12 oxygens. The Fe^{2+}/Fe^{3+} was calculated assuming full occupancy. The chemical formulae of detrital tourmalines were calculated based on 15 Y + Z + T cations, $^{W}O^{2-}$ was obtained from the charge-balanced formula and OH was calculated as OH = 4 – Cl – ^{W}O apfu. B_2O_3 was calculated assuming 3.0 B apfu and H_2O was calculated by considering OH + O + F + Cl apfu. The analyses of detrital Cr-rich spinels were calculated based on 3 cations and Fe^{2+} and Fe^{3+} were allocated according to the ideal stoichiometry.

Results

Heavy mineral assemblages

The dominant heavy mineral in the JAR-2A, B, C samples is garnet (36–69 %) followed by apatite (11–25 %), tourmaline (6–27 %), rutile (6–9 %) and zircon (1–5 %). Subordinate is Cr-rich spinel, epidote and chloritoid (~1 %). In the samples from the Malinowa Fm. garnet (41–59 %) and rutile (23–34 %) are dominant heavy minerals with lesser amount of ultra-stable zircon (10–13 %) and tourmaline (3–8 %). Compared to the samples of the Jarmuta-Proč Fm. the amount of Cr-rich spinel is slightly higher ~3 %, while apatite is much less present (1–3 %). The ZTR index (Hubert, 1962) indicates moderate maturity and is slightly higher in the samples from the Malinowa Fm. (Tab. 2).

Garnets occur mostly as subangular to subrounded grains showing extensive signs of corrosion. Corrosive features include etched facets and etch-pits. Ultra-stable zircon, tourmaline and rutile occur as angular to subrounded grains. Rounded grains were very rare. The ultra-stable minerals show initial to advanced corrosion, especially in tourmaline grains. Apatite is preserved in a form of short subhedral to subrounded grains with incipient signs of corrosion indicating their detrital origin. Cr-rich spinels represent angular to subrounded dark brown, red brown or almost black unaltered fragments. Sporadically preserved minerals such as epidote and chloritoid display advanced signs of corrosion.

Chemical composition of garnets

Almandine-rich garnets with variable grossular, pyrope, and spessartine proportions dominate the examined garnet population in both formations (Fig. 4, Supplementary Tab. S1). Most of the analysed garnets lack inclusions or distinct optical zonation. In few cases inclusions of quartz were observed. The garnet population is slightly more diversified in the Jarmuta-Proč Fm. than in the Malinowa Fm., particularly with more variable grossular molecule proportions (Fig. 4). In the Jarmuta-Proč Fm. the almandine-pyrope garnets with low content of grossular and spessartine ($Alm_{69–85}$ $Prp_{10–25}$ $Grs_{<10}$, $Sps_{<10}$) are the most frequent. These garnets could originate in mica-schists, gneisses metamorphosed under amphibolite or transitional granulite to amphibolite facies conditions. The second group involves almandine-spessartine garnets with low pyrope and grossular molecules ($Alm_{72–77}$ $Sps_{10–40}$ $Prp_{6–14}$ $Grs_{<10}$). Such garnets might come from granitoids (Mange & Morton, 2007). The third group comprises garnets with higher grossular molecule and with variable pyrope and spessartine molecules ($Alm_{55–81}$ $Grs_{11–30}$ $Prp_{1–18}$ $Sps_{1–23}$). Their source rocks might be amphibolites.

In the Malinowa Fm., the almandine-pyrope and almandine-spessartine garnets are the most frequent garnets as well. Here, garnets with higher proportion of grossular can be divided into two groups either with high pyrope and low spessartine ($Alm_{59–73}$ $Grs_{10–20}$ $Prp_{14–27}$ $Sps_{<2}$) or with increased spessartine and low-pyrope molecule (Alm_{57} Grs_{26} Sps_{12} Prp_5). The former could originate in more basic metamorphic rocks metamorphosed under higher amphibolite and/or transitional amphibolite to granulite facies conditions, the latter could come from gneisses or amphibolites metamorphosed under lower amphibolite facies conditions.

Chemical composition of tourmalines

Analysed tourmalines display complex optical zoning (Fig. 5). Altogether 74 analyses, representing spot analyses placed in distinct optical zones were carried out to reveal possible changes in chemical compositions indicative of their evolution (Supplementary Tab. S2). Any obvious distinction in chemical compositions between the studied formations has been observed. Based on the dominant occupancy of the X site most of the tourmalines belong to the X-vacant group, less to the alkali group and few tourmalines belong to the calcic group (Fig. 6A). The X-vacant tourmalines have moderate number of vacancies and display magnesio-foititic to foititic compositions (Fig. 6B). The alkaline tourmalines have dravitic-schorlitic compositions (Fig. 6B, Supplementary Tab. S2). Two

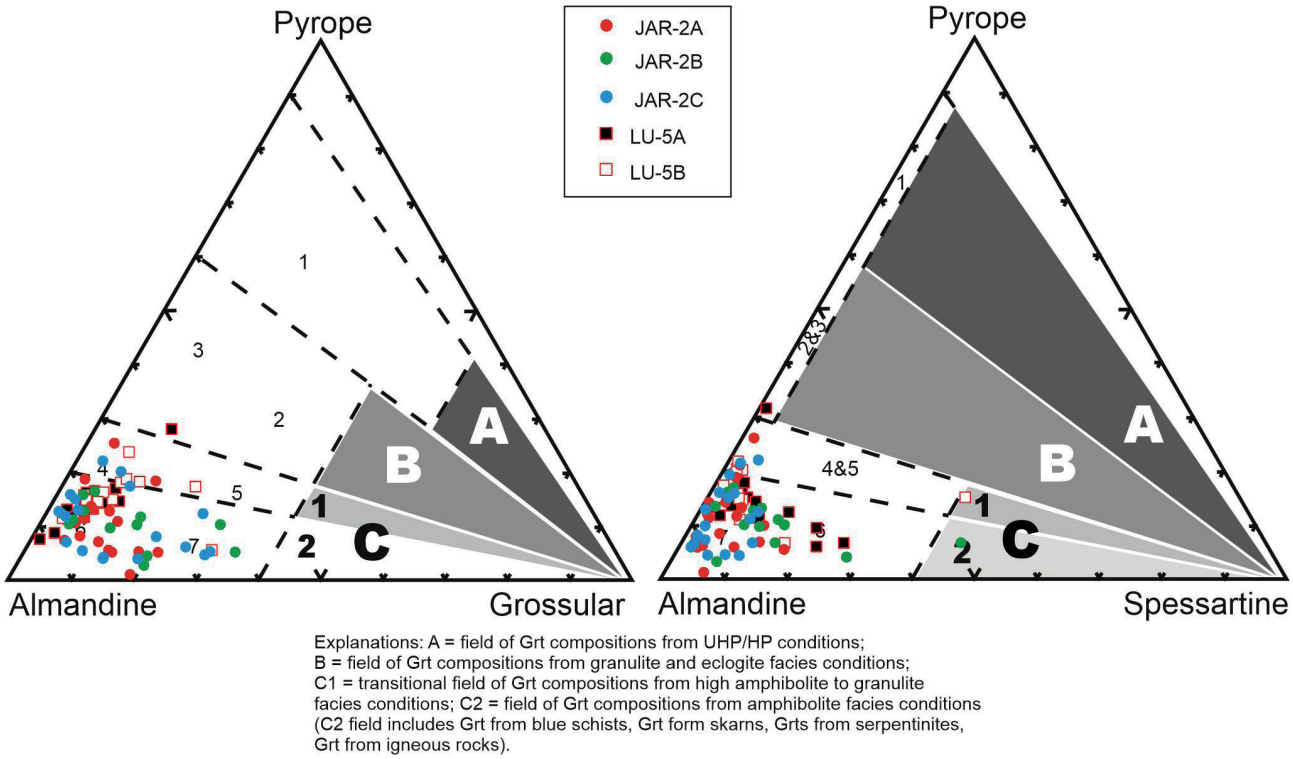

Fig. 4. Triangular pyrope-almandine-grossular and pyrope-almandine-spessartine discrimination diagrams for garnets (after Méres, 2008; Aubrecht et al., 2009)

calcic tourmalines show uvite to feruvite compositions (Fig. 6C). The magnesio-foititic and foititic tourmalines forms either cores of grains, oscillatory zones or optically distinct complex zones and rims (Fig. 5A, B, C, D, G). Some grains or zones of dravitic-schorlitic composition show fine complex intergrowths with quartz, which often overgrow the cores or zones of magnesio-foititic to foititic tourmalines (Fig. 5B, D, E). Zones of dravitic-schorlitic compositions contain abundant mineral inclusions represented by quartz, rutile, zircon, monazite, ilmenite, apatite, allanite, albite and Fe-oxides (Fig. 5B, D, E). Some of the tourmaline grains with distinct optical zonations do not show compositional variations (Fig. 5F, G).

Sources of the analysed tourmalines represent mostly metasedimentary rocks both coexisting and not coexisting with Al-saturation phase and iron-rich quartz-tourmaline, calc-silicate rocks and metapelites (Fig. 7A). Lesser number of tourmalines could originate also in Li-poor granitoids and associated pegmatites and aplites. In the Fe_{tot}-Mg-Ca diagram (Henry & Guidotti, 1985) the analysed tourmalines plot mostly in the fields of Ca-poor metasedimentary rocks, less in the field of Li-poor granitoids and related pegmatites and aplites (Fig. 7B).

Chemical composition of Cr-rich spinels

In total, 26 detrital Cr-rich spinels were analysed (Supplementary Tab. S3). The analysed Cr-rich spinels do not show signs of alteration or zonation (Fig. 5). The Al_2O_3 content vary in the samples from the Jarmuta-Proč Fm. in the narrow range 22.31 to 26.87 wt % and TiO_2 content is very low < 0.11 wt % (Fig. 8A). In the samples from the Malinowa Fm., the Al_2O_3 and TiO_2 contents are more variable in the range 6.04 to 39.10 and < 0.41 wt %, respectively (Fig. 8A). Only few spinel grains from the Malinowa Fm. have the TiO_2 concentrations higher than 0.2 wt % (Fig. 8A), which point to their origin in volcanic rocks (Lenaz et al., 2000; Kamenetsky et al., 2001). The volcanic spinels correspond mostly to the compositions of arc and/or back-arc basin basalts (Fig. 8A). Rare inclusions observed in the volcanic spinels consist of clinopyroxene with diopside composition (Supplementary Tab. S4).

Almost all analysed Cr-rich spinels in both formations have the Fe^{2+}/Fe^{3+} ratio higher than 4, what is characteristic for mantle peridotites (Lenaz et al., 2000; Kamenetsky et al., 2001). Analysis of occasional mineral inclusions in the Cr-rich spinels from peridotites showed that they consist of orthopyroxene with composition of Mg-rich enstatite end-member (Supplementary Tab. S4). The Cr# and Mg# in the samples from the Jarmuta-Proč Fm. were ~0.5 and ~0.6, respectively. In the Malinowa Fm., the Cr# and Mg# vary between 0.32 to 0.87 and 0.35 to 0.69, respectively. In the Cr# vs. Mg# diagram (Pober & Faupl, 1988), the analysed Cr-rich spinels best match the harzburgite field and/or podiform chromitite field (Fig. 8B).

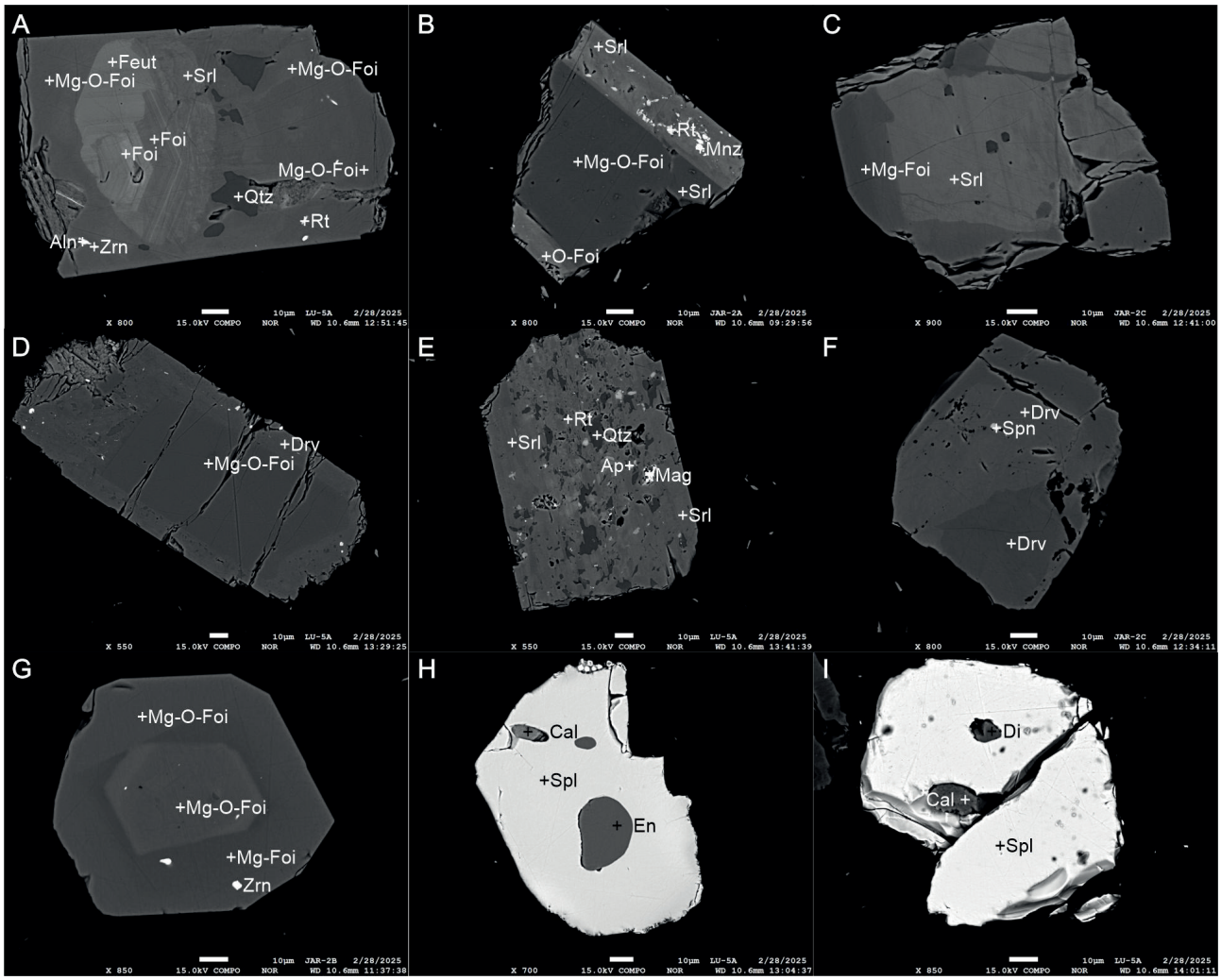

Fig. 5. BSE images of the analysed detrital tourmalines (A – G) and Cr-rich spinels (H, I). The tourmalines show distinct optical zoning often with contrasting chemistry. The Cr-rich spinels, either of peridotitic (H) or volcanic origin (I), show no signs of alteration or zonations. Abbreviations after (Whitney & Evans, 2010) except for tourmaline species where: Foi – foitite, Feut – feruvite; Mg-O-Foi – "magnesio-oxy-foitite"; Fe-O-Foi – "oxy-foitite"

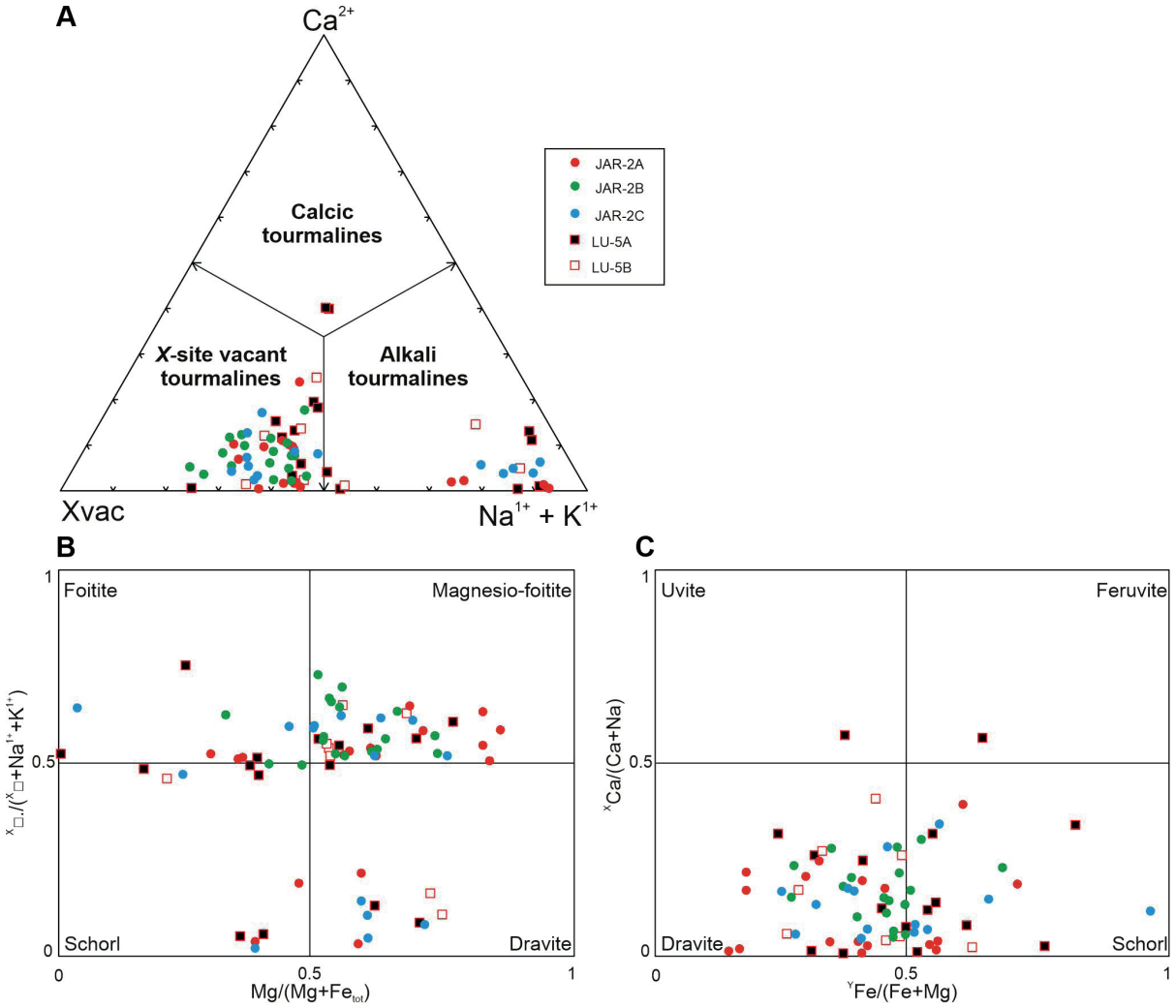

Fig. 6. A) Ternary system for the primary tourmaline groups based on the dominant occupancy of the X site; B) binary classification diagram for establishing the appropriate tourmaline subgroups in the alkali and X-vacant groups; C) binary classification diagram for establishing the appropriate tourmaline subgroups in the calcic group (according to Henry et al., 2011)

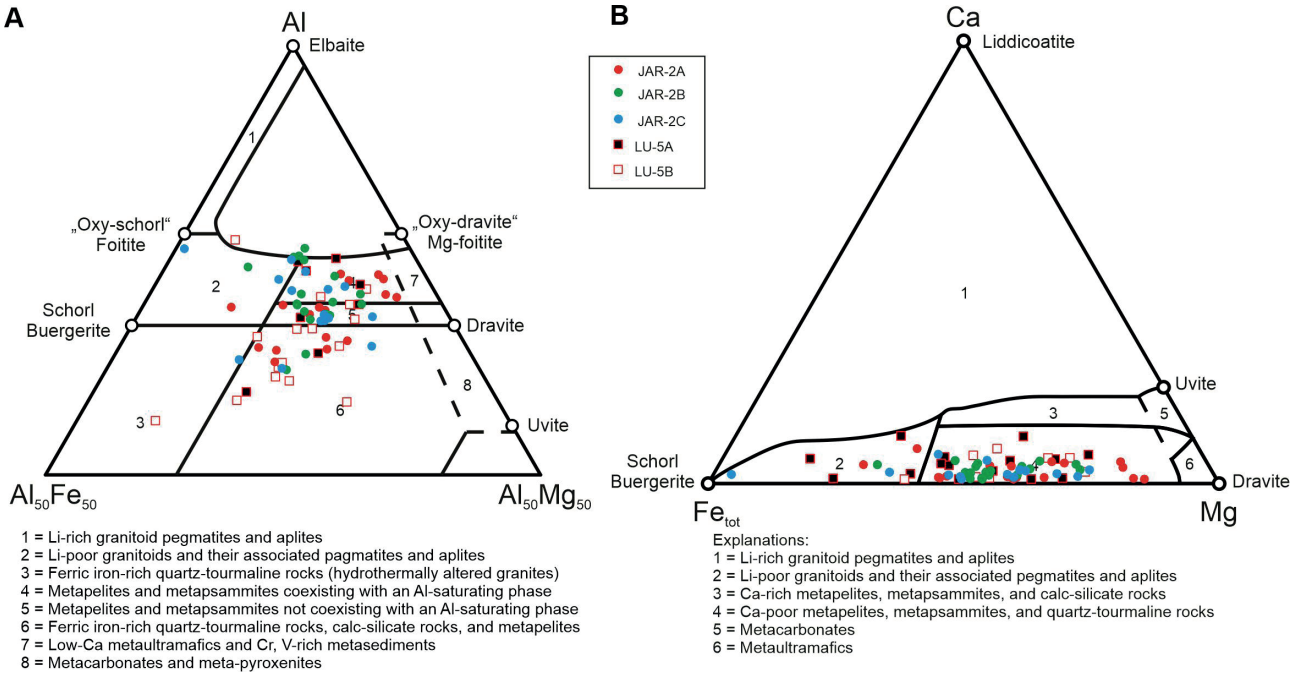

Fig. 7. Triangular Al-$Al_{50}Fe_{50}$-$Al_{50}Mg_{50}$ diagram in A) and Ca-Fe_{tot}-Mg diagram in B) (in molar proportions) discriminating tourmalines originated in various rock types (after Henry & Guidotti, 1985)

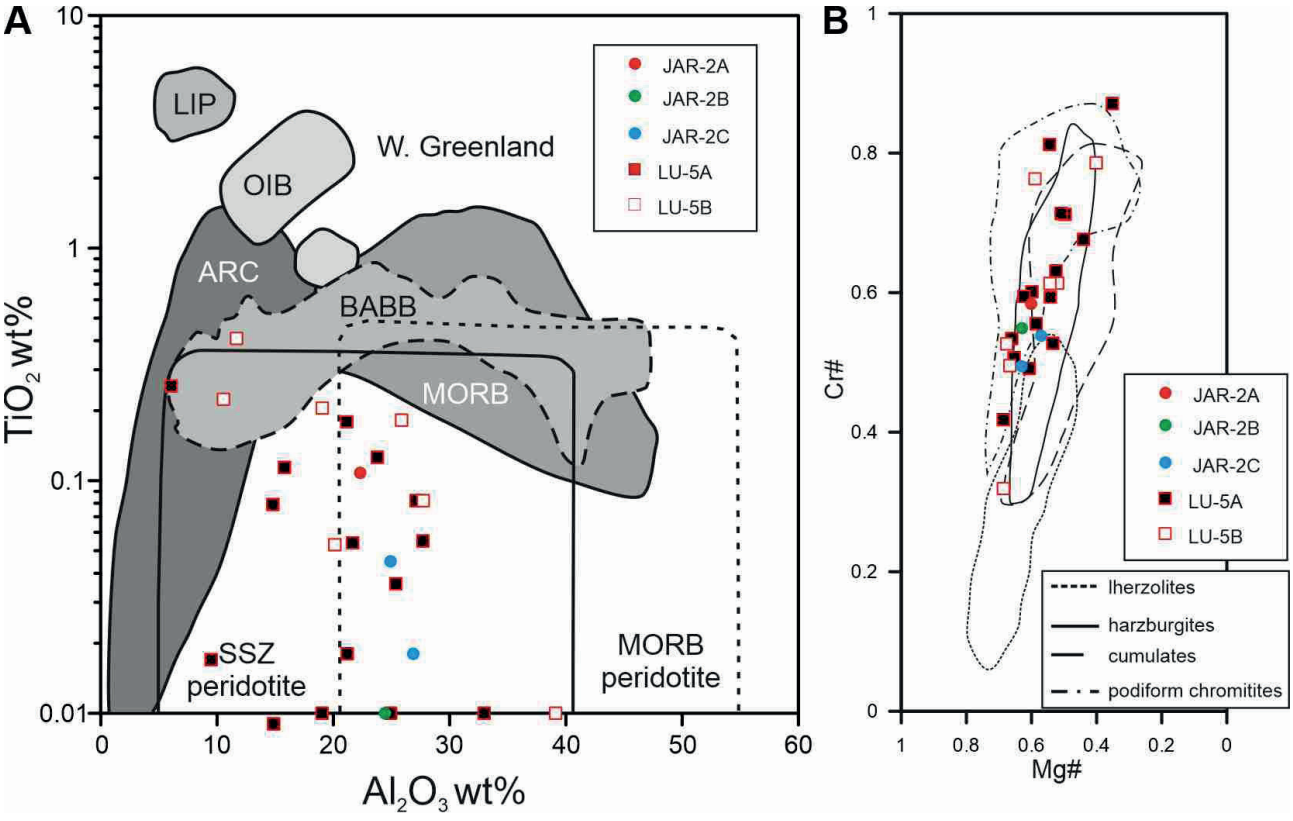

Fig. 8. A) The Al_2O_3 vs. TiO_2 diagram with Cr-rich spinel discrimination fields (after Kamenetsky et al., 2001). Explanations: SSZ = supra-subduction zone, MORB = mid-ocean ridge basalts, BABB = back-arc basin basalts, ARC = island-arc magmas, OIB = ocean-island basalts, LIP = large igneous province. B) The Cr# versus Mg# diagram for Cr-rich spinels (Pober & Faupl, 1988)

Discussion

Provenance of garnets

Garnet is the most frequent heavy mineral in both studied formations (Tab. 2). It fits the reported increasing garnet contents in the Upper Cretaceous to Lower Eocene synorogenic deposits of the PKB (Salata, 2004; Oszczypko & Salata, 2005; Aubrecht et al., 2009, 2020a, 2021; Bónová et al., 2018; Madzin et al., 2019). The increasing trend has been attributed to a new influx of garnets and associated heavy minerals, especially apatite and rutile, from continental metamorphic and magmatic rocks (Aubrecht et al., 2021). Chemical analyses of detrital garnets showed that almandine-rich garnets prevail. The garnet population is slightly more diverse in the Jarmuta-Proč Fm. than in the Malinowa Fm., which might indeed reflect the new input of garnets from medium-grade basic metamorphic rocks during the latest Cretaceous. Almandine is the most frequent garnet type observed in the Upper Cretaceous to Lower Eocene clastic formations throughout the PKB (Salata, 2004; Oszczypko & Salata, 2005; Aubrecht et al., 2009, 2020a, 2021; Bónová et al., 2018; Madzin et al., 2019). Garnets with high content of pyrope molecule ($Prp_{>30}$), derived from eclogites or mafic granulites, reported from the Jarmuta-Proč Fm. of the more eastern part of the PKB (Madzin et al., 2019) or from the Turonian Snežnica Fm. of the Kysuca (Pieniny) Unit of the Orava sector (Aubrecht et al., 2021) were not observed in our examined material. The analysed garnets were derived mostly from low- to mid-/high-grade polymetamorphic terrains. Some of the almandine-rich garnets could also come from granitoid rocks (cf. Oszczypko & Salata, 2005; Bónová et al., 2018; Madzin et al., 2019).

The almandine garnets with the low pyrope, higher grossular and variable spessartine molecule proportions ($Alm_{>55}$ $Grs_{12–30}Prp_{<5}Sps_{1–24}$) are similar to almandine-dominated garnets described recently from a blueschist-facies metabasite pebble of the Albian-Cenomanian exotics-bearing conglomerates of the Peri-Klippen Klape Unit and from the HP/LT metamorphosed Bôrka Nappe of the Meliata Unit (Putiš et al., 2023). The dating revealed their almost identical Late Jurassic Lu-Hf garnet ages of 152.1 ± 1.5 Ma and 153.95 ± 0.69 Ma, respectively, and comparable P-T metamorphic conditions (Putiš et al., 2023). Accordingly, a part of the detrital garnets might have been derived from the Meliata Unit originally deposited in mid-Cretaceous flysch of the Fatric Klape or analogous units and then resedimented into the Upper Cretaceous to Eocene Jarmuta-Proč Fm. (see e.g., Plašienka et al., 2019).

Provenance of tourmalines

Detrital tourmalines represent one of the most frequent transparent heavy minerals in the Upper Cretaceous to Lower Eocene flysch deposits of the PKB and neighbouring Peri-Klippen Zone (Oszczypko & Salata, 2005; Bellová et al., 2018; Bónová et al., 2018; Madzin et al., 2019; Aubrecht et al., 2020a, 2020b, 2021; Madzin & Plašienka, 2022). The presented chemical compositions of detrital tourmalines from the Malinowa and Jarmuta-Proč Fms. reveal their derivation mostly from low- to medium-grade metamorphic rocks and to a lesser extent also from granitoid rocks (Fig. 7). Distinct optical zoning with very often contrasting chemistry points to a complex polymetamorphic history of the analysed tourmalines. Recently, heavy mineral analyses of the mid- to Late Cretaceous exotics-bearing formations of the Central Western Carpathians (CWC) and PKB revealed considerable amounts of complex-zoned tourmalines that could have been derived from decompressed (exhumed) HP/LT ultramafic rocks of the Meliata ophiolite-bearing complexes (Bellová et al., 2018; Plašienka et al., 2019; Aubrecht et al., 2020a, 2020b, 2021). The poikiloblastic "mosaic" tourmalines with obvious bosiite trend (Bačík et al., 2018; Aubrecht et al., 2020b) have not been observed in our sampled material, but similar complex-zoned magnesio-foititic to foititic and schorlitic-dravitic tourmalines with fine intergrowth with quartz and abundant mineral inclusions represent the dominant types in the deposits studied (Fig. 5). Such magnesio-foititic to foititic tourmalines have not been detected in the previous heavy mineral studies of the Jarmuta-Proč Fm., where optically zoned tourmalines show only dravitic-schorlitic compositions (Oszczypko & Salata, 2005; Madzin et al., 2019). Similar magnesio-foititic to foititic tourmalines were recently found also in the Upper Cretaceous-Paleocene turbiditic deposits of the Pupov Fm. from the Peri-Klippen Zone of the Kysuca sector of the PKB (Madzin & Plašienka, 2022). The magnesio-foititic to foititic tourmalines are quite unusual, however their primary occurrences have already been described from the CWC in alpine-type hydrothermal veins cutting the crystalline basement rocks of the Tatric (Uher et al., 2009) and Gemeric units (Bačík et al., 2017, 2018). The distribution of the hydrothermal veins has been, however, considered to be limited as an important regional source for the complex-zoned tourmalines (Aubrecht et al., 2020a, 2020b). More probably, the complex-zoned tourmalines might come from the HP/LT ultramafic rocks of the Meliata ophiolite-bearing complexes (Bellová et al., 2018; Aubrecht et al., 2020a, 2020b; Plašienka et al., 2019). The apparent controversy related to their presence in the flysch formations deposited on the other (external) side of the orogenic belt and their derivation from the distant southern Western Carpathian zones can be explained by a multiple recycling model as proposed for the derivation of ophiolitic debris in the Cretaceous to Paleogene flysch formations of the CWC and PKB (Plašienka, 2012a and references therein). The Meliata

ophiolite-bearing complexes were exposed to erosion during the Lower Cretaceous in the southern Western Carpathian zones and the ophiolitic debris together with the "exotic" pebble material was primarily deposited in the Albian-Cenomanian flysch deposits of the Poruba Fm. in the Fatric Zliechov Basin (Plašienka, 1995a, 1995b, 1996; Plašienka, 2012a). The Poruba Fm. was, as a part of the Fatric nappe system, emplaced during the Late Turonian into a false accretionary wedge position behind the outer Tatric margin, thereby becoming a part of the Klape Unit in the Peri-Klippen Zone (Plašienka, 1995a, 1995b, 1996, 2012a; Prokešová et al., 2012; Plašienka et al., 2019). In such way, the mid-Cretaceous flysch formations of the Klape Unit, already incorporated into the developing accretionary wedge, could form the "proximal" source of ophiolitic debris and complex-zoned tourmalines for still younger synorogenic deposits in the foredeep basins of the PKB and adjoining zones (Plašienka, 2012a; Plašienka & Soták, 2015; Plašienka et al., 2019; Madzin & Plašienka, 2022). The poor roundness of tourmaline grains may intuitively look contradictory to their supposed recycled origin in the parental Klape/Poruba flysch formations. However, tourmaline represents one of the ultra-high stable minerals, which can survive multiple sedimentary cycles (Hubert, 1962; Morton & Hallsworth, 1999, 2007), and unlike to pebbles in gravel, which are prone to rounding, abrasion of psammitic fraction is a very slow and ineffective process during transport in aqueous conditions (e.g., Garzanti, 2017).

Provenance of Cr-rich spinels

Significant amounts of Cr-rich spinels with decreasing-upward trend were found in the Upper Cretaceous to Lower Eocene flysch deposits of the PKB (Winkler & Ślączka, 1992, 1994; Salata, 2004; Oszczypko & Salata, 2005; Bónová et al., 2018; Madzin et al., 2019; Aubrecht et al., 2009, 2020a, 2021). Comparison of Cr-rich spinel contents between the Turonian-Campanian Malinowa Fm. of the Šariš Unit and contemporaneous Turonian-Santonian Snežnica and Sromowce Fms. of the Kysuca (Pieniny) Unit (Aubrecht et al., 2021) shows the obvious depletion of ophiolitic debris in the former. It might be attributed to a more distal position of the Šariš Basin, where the Malinowa Fm. was deposited, compared to a proximal position of the Pieniny Basin, where turbiditic sandstones and conglomerates of the Snežnica and Sromowce Fms. received large amounts of ophiolitic debris and polymict pebble material during the Late Cretaceous (cf. Plašienka, 2012a).

The chemical compositions of the analysed Cr-rich spinels point to their origin predominantly in supra-subduction zone peridotites of harzburgitic composition and sporadically also in volcanic rocks (cf. Oszczypko & Salata, 2005; Aubrecht et al., 2009, 2020a, 2021; Bónová et al., 2018; Madzin et al., 2019). The source of the ophiolitic detritus in the Upper Cretaceous clastic deposits of the PKB has been generally considered to be the same as for the material of the exotics-bearing Albian-Cenomanian conglomerates of the Klape Unit (Mišík & Marschalko, 1988; Dal Piaz et al., 1995; Kissová et al., 2005; Aubrecht et al., 2009; Plašienka, 2012a). Although, the origin, paleogeographic position and interpretation of the Klape Unit is a subject of decades-lasting debates, there exists a consensus, that the ophiolitic detritus comes from the Neotethyan Meliata ophiolite-bearing complexes situated in the southern Western Carpathian zones (for comprehensive review see recent works by Aubrecht et al., 2009; Plašienka, 2012a; Bellová et al., 2018; Plašienka et al., 2019; Aubrecht, et al., 2020a, 2020b, 2021). Interestingly, Cr-rich spinels from serpentinized peridotite bodies of the Meliata ophiolite-bearing complexes show mostly lherzolitic composition (Mikuš & Spišiak, 2007). In contrast, detrital Cr-rich spinels from harzburgitic sources dominate in the Upper Jurassic to Cretaceous synorogenic formations throughout the whole Alpine-Carpathian-Dinaridic orogenic system (Pober & Faupl, 1988; Mikes et al., 2008; Lužar-Oberiter et al., 2009; Gawlick et al., 2015; Bellová et al., 2018; Aubrecht et al., 2020a). The source of harzburgitic Cr-rich spinels has been interpreted to be in obducted Jurassic Neotethyan ophiolites predominantly of harzburgitic composition (Gawlick et al., 2015, 2020), situated in a higher nappe position over the older almost completely subducted Triassic Neotethyan ocean floor predominantly of lherzolitic composition (e.g., Bortolotti et al., 2013). The ophiolitic nappe stack is however missing in the Western Carpathians and its existence may be witnessed only in polygenetic ophiolite-bearing mélanges (Plašienka et al., 2019; Molčan Matejová et al., 2025), while pure ophiolitic mélanges below overriding ophiolite nappes are well-preserved in the Dinaric-Hellenic orogenic belt (e.g., Gawlick & Missoni, 2019 and references therein).

The original concept assumed the source of the exotic material in an exotic ridge, known as the Pieniny or the Andrusov Ridge (Mišík & Sýkora, 1981; Birkenmajer, 1988; Mišík & Marschalko, 1988). The Andrusov Ridge should have been situated between the Oravic-Vahic sedimentary realm and the CWC domain and was interpreted as an accretionary wedge, formed by the subduction of the South Penninic Vahic Ocean (in sense of Maheľ, 1981, 1989; Birkenmajer, 1988). However, the age and composition of the exotic conglomerates, dominantly of "southern" Meliata-related origin, is inconsistent with the Upper Jurassic to Lower Cretaceous structural, magmatic and sedimentary record from the external Tatric margin (Plašienka, 1995a, 1995b, 1996, 2012a). Consequently, the Klape flysch formations were interpreted to be an analogue to the Albian-Cenomanian

Poruba flysch formations of the Tatric and Fatric units of the CWC, situated in a false accretionary wedge position where they formed the source of ophiolitic debris recycled to younger sediments of the foreland basins of the PKB (as described in *Provenance of tourmalines* section above) (Plašienka, 1995a, 1995b, 1996, 2012a; Plašienka et al., 2019). The high vs low Cr-rich spinel content in proximal vs distal Turonian-Campanian deposits of the Pieniny and Šariš Basins, respectively, might support the multiple recycling model as well.

Another model explaining how the Meliata ophiolite-bearing complexes could become the source for the ophiolitic debris and exotic conglomerates of the PKB (Aubrecht et al., 2009; Bellová et al., 2018; Aubrecht et al., 2020a). In this model, the Oravic crustal segment originally formed a lateral continuation of the CWC, and both units were situated north of the Meliata oceanic realm (e.g., Michalík, 1994; Aubrecht et al., 2009). After the closure of the Meliata Ocean in the Late Jurassic, the Meliata suture zone was welded to the southern (internal) parts of both the CWC and Oravic segment. Later during the Cretaceous, the Meliata ophiolite complex was secondarily doubled by a left-lateral shift of the Oravic crustal segment along the northern (external) margin of the CWC block due to its clockwise rotation (Aubrecht & Túnyi, 2001). A long-lived elevation, the Andrusov Ridge, formed within a complex shear zone between the two rotated crustal segments (e.g., Rakús & Marschalko, 1997; Marschalko & Rakús, 1997). In this way, the Andrusov Ridge could feed the Cretaceous clastic formations of both the CWC and PKB units with pebble material and ophiolitic detritus for a long time (Aubrecht et al., 2009, 2020a; Bellová et al., 2018). However, structural arguments for such movements of the Oravic segment have not yet been presented and the new paleomagnetic data proved that the large clockwise rotation of the CWC block is younger than the Late Turonian-Santonian (Grabowski, 2000; Márton et al., 2020; Madzin et al., 2026).

Conclusions

The heavy mineral analysis and detrital garnet, tourmaline and Cr-rich spinel chemical compositions from fine-grained turbiditic sandstones of the Maastrichtian-Ypresian Jarmuta-Proč Fm. (samples from the borehole Jar-2) and from fine-grained sandstones of the hemipelagic Turonian-Campanian Malinowa Fm. (samples from outcrop) of the Šariš Unit of the Pieniny Klippen Belt in eastern Slovakia showed that:

1. Almandine-rich garnets with variable grossular, pyrope, and spessartine proportions dominate the examined garnet population in both formations. The analysed garnets were derived mostly from low- to medium/high-grade polymetamorphic terrains. The slightly more diverse garnet population of the Jarmuta-Proč Fm. might reflect a new input of garnets from medium-grade, prevailingly basic metamorphic rocks during the latest Cretaceous. Some of the almandine-rich garnets could come from granitoid rocks.
2. Distinct optical zoning with very often contrasting chemistry point to a complex polymetamorphic history of the analysed tourmalines. The unusual complex-zoned tourmalines are represented mostly by X-vacant magnesio-foititic to foititic and schorlitic-dravitic tourmalines with fine intergrowths with quartz and abundant mineral inclusions.
3. Most of the analysed Cr-rich spinels in both studied formations show chemistry typical for supra-subduction zone peridotites. Sporadic volcanic spinels correspond to the compositions of arc and/or back-arc basin basalts.
4. The chemistry of the Cr-rich spinels and complex-zoned tourmalines supports their common provenance in the Meliata ophiolite-bearing complexes of the internal Western Carpathian zones.
5. The decreasing-upward Cr-rich spinel contents in the Upper Cretaceous to Lower Eocene flysch deposits of the PKB is evident. A multiple recycling model in which the Klape flysch formations situated in a false accretionary wedge position formed the "proximal" source of ophiolitic debris recycled to the younger flysch formations of the foreland basins is advocated.

Acknowledgements

This study was financially supported by projects APVV-20-0079, 21-0281, Vega 2/0013/20, 2/0171/24, 2/0012/24, 1/0021/25. Tomáš Mikuš and Sergii Kurylo are appreciated for their help during EMPA analyses. The authors are grateful to reviewers and the editor for comments and suggestions, which helped to improve the paper.

References

Aubrecht, R. & Túnyi, I., 2001: Original orientation of neptunian dykes in the Pieniny Klippen Belt (Western Carpathians): the first results. *Contributions to Geophysics and Geodesy*, 31, 3, 557–578.

Aubrecht, R., Méres, Š., Sýkora, M. & Mikuš, T., 2009: Provenance of the detrital garnets and spinels from the Albian sediments of the Czorsztyn Unit (Pieniny Klippen Belt, Western Carpathians, Slovakia*). Geologica Carpathica*, 60, 463–483.

Aubrecht, R., Bellová, S. & Mikuš, T., 2020a: Provenance of Albian to Cenomanian exotics-bearing turbidites in the Western Carpathians: a heavy mineral analysis. *Geological Quarterly*, 64, 3, 658–680.

Aubrecht, R., Bačík, P., Mikuš, T. & Bellová, S., 2020b: Detritic tourmalines with complex zonation in the Cretaceous

exotic flysches of the Western Carpathians: Where did they come from? *Lithos*, 362–363, 105443.

Aubrecht, R., Mikuš, T. & Holický, I., 2021: Heavy mineral analysis of the Turonian to Maastrichtian exotics-bearing deposits in the Western Carpathians: What has changed after the Albian and Cenomanian? *Geologica Carpathica*, 72, 505–528.

Bačík, P., Dikej, J., Fridrichová, J., Miglierini, M. & Števko, M., 2017: Chemical composition and evolution of tourmaline-supergroup minerals from the Sb hydrothermal veins in Rožňava area, Western Carpathians. Slovakia. *Mineralogy and Petrology*, 111, 609–624.

Bačík, P., Uher, P., Dikej, J. & Puškelová, Ľ., 2018: Tourmalines from the siderite-quartz-sulphide hydrothermal veins, Gemeric unit, western Carpathians, Slovakia: crystal chemistry and evolution. *Mineralogy and Petrology*, 112, 45–63.

Bellová, S., Aubrecht, R. & Mikuš, T., 2018: First results of systematic provenance analysis of the heavy mineral assemblages from the Albian to Cenomanian exotic flysch deposits of the Klape Unit, Tatricum, Fatricum and some adjacent units. *Acta Geologica Slovaca*, 10, 1, 45–64.

Birkenmajer, K., 1977: Jurassic and Cretaceous lithostratigraphic units of the Pieniny Klippen Belt, Carpathians, Poland. *Studia Geologica Polonica*, 45, 1–158.

Birkenmajer, K., 1986: Stages of structural evolution of the Pieniny Klippen Belt, Carpathians. *Studia Geologica Polonica*, 88, 7–32.

Birkenmajer, K., 1988: Exotic Andrusov Ridge: its role in plate--tectonic evolution of the West Carpathian foldbelt. *Studia Geologica Polonica,* 41, 7–37.

Bortolotti, V., Chiari, M., Marroni, M., Pandolfi, L., Principi, G. & Saccani, E., 2013: Geodynamic evolution of ophiolites from Albania and Greece (Dinaric-Hellenic belt): one, two, or more oceanic basins? *International Journal of Earth Sciences*, 102, 783–811. https://doi.org/10.1007/s00531-012-0835-7.

Bónová, K., Mikuš, T. & Bóna, J., 2018: Is Cr-spinel geochemistry enough for solving the provenance dilemma? Case study from the Palaeogene sandstones of the Western Carpathians (eastern Slovakia). *Minerals*, 8, 543. https://doi.org/10.3390/min8120543.

Dal Piaz, G. V., Martin, S., Villa, M. I., Gosso, G. & Marschalko, R., 1995: Late Jurassic blueschist pebbles from the Western Carpathian orogenic wedge and paleostructural implications for Western Tethys evolution. *Tectonics*, 14, 4, 8974–885.

Galehouse, J. S., 1971: Point counting. In: Carver, R. E. (ed.): Procedures in Sedimentary Petrology. *New York, Wiley InterScience*, 385–407.

Garzanti, E., 2017: The maturity myth in sedimentology and provenance analysis. *Journal of Sedimentary Research*, 87, 353–365. https://doi.org/10.2110/jsr.2017.17.

Gawlick, H.-J. & Missoni, S., 2019: Middle-Late Jurassic sedimentary mélange formation related to ophiolite obduction in the Alpine-Carpathian-Dinaridic Mountain Range. *Gondwana Research*, 74, 144–172. https://doi.org/10.1016/j.gr.2019.03.003.

Gawlick, H.-J., Aubrecht, R., Schlagintweit, F., Missoni, S. & Plašienka, D., 2015: Ophiolitic detritus in Kimmeridgian resedimented limestones and its provenance from an eroded obducted ophiolitic nappe stack south of the Northern Calcareous Alps (Austria). *Geologica Carpathica*, 66, 6, 473–487.

Gawlick, H.-J., Sudar, M., Missoni, S., Aubrecht, R., Schlagintweit, F., Jovanović, D. & Mikuš, T., 2020: Formation of a Late Jurassic carbonate platform on top of the obducted Dinaridic ophiolites deduced from the analysis of carbonate pebbles and ophiolitic detritus in southwestern Serbia. *International Journal of Earth Sciences*, 109, 2023–2048. https://doi.org/10.1007/s00531-020-01886-w.

Golonka, J., Krobicki, M., Waśkowska, A., Cieszkowski, M. & Ślączka, A., 2015: Olistostromes of the Pieniny Klippen Belt, Northern Carpathians. *Geological Magazine*, 152, 269–86.

Grabowski, J., 2000: Palaeo- and rock magnetism of Mesozoic carbonate rocks in the Sub-Tatric series (Central West Carpathians) – palaeotectonic implications. *Polish Geological Institute, Special Papers*, 5, 1–88.

Henry, D. J. & Guidotti, C. V., 1985: Tourmaline as a petrogenetic indicator mineral: an example from the staurolite-grade metapelites of NW Maine. *American Mineralogist*, 70, 1–15.

Henry, D. J., Novák, M., Hawthorne, F. C., Ertl, A., Dutrow, B. L., Uher, P. & Pezzotta, F., 2011: Nomenclature of the tourmaline-supergroup minerals. *American Mineralogist*, 96, 895–913.

Hubert, F. J., 1962: A zircon-tourmaline-rutile maturity index and the interdependence of the composition of heavy mineral assemblages with the gross composition and texture of sandstones. *Journal of Sedimentary Petrology*, 32, 3, 440–450.

Jurewicz, E., 1997: The contact between the Pieniny Klippen Belt and Magura Unit (the Małe Pieniny Mts.). *Geological Quarterly*, 41, 315–326.

Jurewicz, E., 2005: Geodynamic evolution of the Tatra Mts. and the Pieniny Klippen Belt (Western Carpathians): problems and comments. *Acta Geologica Polonica*, 55, 295–338.

Jurewicz, E., 2018: The Šariš Transitional Zone, revealing interactions between Pieniny Klippen Belt, Outer Carpathians and European platform. *Swiss Journal of Geosciences*, 111, 245–267.

Kamenetsky, V. S., Crawford, A. J. & Meffre, S., 2001: Factors controlling chemistry of magmatic spinel: an empirical study of associated olivine, Cr-spinel and melt inclusion from primitive rocks. *Journal of Petrology*, 42, 655–671.

Kissová, D., Dunkl, I., Plašienka, D., Frisch, W. & Marschalko, R., 2005: The Pieninic exotic cordillera (Andrusov Ridge) revisited: new zircon FT ages of granite pebbles from Cretaceous conglomerates of the Pieniny Klippen Belt (Western Carpathians, Slovakia). *Slovak Geological Magazine*, 11, 17–28.

Kováč, P. & Hók, J., 1996: Tertiary development of the western part of Klippen Belt. *Slovak Geological Magazine*, 2, 136–149.

Lenaz, D., Kamenetsky, V. S., Crawford, A. J. & Princivalle, F., 2000: Melt inclusion in detrital spinel from the SE Alps (Italy–Slovenia): a new approach to provenance studies

of sedimentary basins. *Contributions to Mineralogy and Petrology*, 139, 748–758. https://doi.org/10.1007/s004100000170.

Ludwiniak, M., 2018: Miocene transpression effects at the boundary of Central Carpathian Paleogene Basin and Pieniny Klippen Belt: examples from Polish-Slovakian borderland. *Geology Geophysics and Environment*, 44, 91–110. https://doi.org/10.7494/geol.2018.44.1.91.

Lužar-Oberiter, B., Mikes, T., von Eynatten, H. & Babić, L., 2009: Ophiolitic detritus in Cretaceous clastic formations of the Dinarides (NW Croatia): evidence from Cr-spinel chemistry. *International Journal of Earth Sciences*, 98, 1097–1108. https://doi.org/10.1007/s00531-008-0306-3.

Madzin, J. & Plašienka, D., 2022: Petrographic and heavy mineral analysis of the Upper Cretaceous – Paleocene turbiditic deposits of the Pupov Formation (Western Carpathians, Pieniny Klippen Belt, Terchová-Zázrivá area). *Acta Geologica Slovaca*, 14, 2, 115–130.

Madzin, J., Plašienka, D. & Méres, Š., 2019: Provenance of synorogenic deposits of the Upper Cretaceous-Lower Palaeogene Jarmuta-Proč Formation (Pieniny Klippen Belt, Western Carpathians). *Geologica Carpathica*, 70, 1, 15–34. https://doi.org/ 10.2478/geoca-2019-0002.

Madzin, J., Márton, E., Plašienka, D. & Imre, G., 2026: A large post-Santonian clockwise rotation of the Central Carpathian nappe stack constrained by new and published paleomagnetic results. *Journal of Geodynamics*, 167, 102135. https://doi.org/10.1016/j.jog.2026.102135.

Maheľ, M., 1981: Island character of the Klippen Belt: Vahicum-continuation of the southern Penninicum in the Western Carpathians. *Geologický Zborník – Geologica Carpathica*, 32, 3, 293–305.

Maheľ, M., 1986: Geological structure of the Czechoslovak Carpathians, Paleoalpine units 1. *Bratislava, Veda,* SAS, 1–503 (in Slovak).

Maheľ, M., 1989: Pieniny Klippen belt from the geodynamic model aspect. *Mineralia Slovaca*, 21, 99–108.

Mange, M. A. & Morton, A. C., 2007: Geochemistry of heavy minerals. In: Mange, M. A. & Wright, D. T. (eds.): Heavy Minerals in Use. Developments in Sedimentology. *Amsterdam, Elsevier*, 345–391.

Marschalko, R., 1986: Development and geotectonic importance of Cretaceous Flysch of the Klippen Belt. *Bratislava, Veda, SAS*, 1–137 (in Slovak with English summary).

Marschalko, R. & Rakús, M., 1997: Development of the Cretaceous flysch in the Klape unit and the recyclicity problem of the clastic material. In: Plašienka, D., Hók, J., Vozár, J. & Elečko, M. (eds.): Alpine Evolution of the Western Carpathians and Related areas. International Conference. Abstracts & Introductory Articles to the Excursion. *Bratislava, Geological Survey of Slovak Republic*, 71–78.

Márton, E., Madzin, J., Plašienka, D., Grabowski, J., Bučová, J., Aubrecht, R. & Putiš, M., 2020: New paleomagnetic constraints for the large-scale displacement of the Hronic nappe system of the Central Western Carpathians. *Journal of Geodynamics*, 1141–142, 101796. https://doi.org/10.1016/j.jog.2020.101796.

Méres, Š., 2008: Garnets – an important information resource about source area and parent rocks of siliciclastic sedimentary rocks. In: Jurkovič, Ľ. (ed.): Conference "Cambelove dni 2008", Abstract Book. *Bratislava, Comenius University*, 37–43 (in Slovak with English Summary).

Michalík, J., 1994: Notes on the Paleogeography and Paleotectonics of the Western Carpathian area during the Mesozoic. *Mitteilungen Österreichischen Geologischen Gessellschaft*, 86, 101–110.

Mikes, T., Christ, D., Petri, R., Dunkl, I., Frei, D., Báldi-Beke, M., Reitner, J., Wemmer, K., Hrvatović, H. & von Eynatten, H., 2008: Provenance of the Bosnian Flysch. *Swiss Journal of Geosciences*, 101, S31–S54. https://doi.org/10.1007/s00015-008-1291-z.

Mikuš, T. & Spišiak, J., 2007: Chemical composition and alteration of Cr-spinels from Meliata and Penninic serpentinized peridotites (Western Carpathians and Eastern Alps). *Geological Quarterly*, 51, 257–270.

Mišík, M., 1997: The Slovak part of the Pieniny Klippen Belt after the pioneering works of D. Andrusov. *Geologica Carpathica*, 48, 4, 209–220.

Mišík, M. & Marschalko, R., 1988: Exotic conglomerates in flysch sequences: Examples from the West Carpathians. In: Rakús, M., Dercourt, J. & Nairn, E. M. A. (eds.): Evolution of the northern margin of Tethys, Vol. 1. *Mémoires de la Société géologique de France, Paris, Nouvelle Série*, 154, 95–113.

Mišík, M. & Sýkora, M., 1981: Pieniny exotic ridge reconstructed from pebbles of carbonate rocks of Cretaceous conglomerates of the Pieniny Klippen Belt and Manín Unit. *Západné Karpaty, Séria Geológia*, 7, 7–111 (in Slovak with English summary).

Molčan Matejová, M., Potočný, T., Plašienka, D. & Aubrecht, R., 2025: Palaeoenvironmental interpretation of chaotic complexes of the Meliata Unit (Western Carpathians, Slovakia): new data from biochronology, lithostratigraphy and geochemistry. *Ofioliti*, 50, 1, 17–36. https://doi.org/10.4454/ofioliti.v50i1.576.

Morton, A. C. & Hallsworth, C. R., 1999: Processes controlling the composition of heavy mineral assemblages in sandstones. *Sedimentary Geology*, 124, 3–29.

Morton, A. C. & Hallsworth, C. R., 2007: Stability of detrital heavy minerals during burial diagenesis. In: Mange, M. A. & Wright, D. T. (eds.): Heavy Minerals in Use. Developments in Sedimentology. *Amsterdam, Elsevier*, 215–245.

Nemčok, M. & Nemčok, J., 1994: Late Cretaceous deformation of the Pieniny Klippen Belt, West Carpathians. *Tectonophysics*, 290, 137–167. https://doi.org/10.1016/0040-1951(94)90109-0.

Nemčok, J., Kullmanová, A. & Ďurkovič, T., 1989: Development and stratigraphic position of the Gregorianka Breccia of the Klippen Belt in eastern Slovakia. *Geologické práce, Správy*, 89, 11–37 (in Slovak).

Oszczypko, N. & Salata, D., 2005: Provenance analyses of the Late Cretaceous-Palaeocene deposits of the Magura basin (Polish Western Carpathians) – evidence from a study of heavy minerals. *Acta Geologica Polonica*, 55, 3, 237–267.

Oszczypko, N., Oszczypko-Clowes, M., Golonka, J. & Marko, F., 2005: Oligocene – Lower Miocene sequences of the Pieniny Klippen Belt and adjacent Magura Nappe between Jarabina and the Poprad River (East Slovakia and

South Poland): their tectonic position and palaeogeographic implications. *Geological Quarterly*, 49, 379–402.

Plašienka, D., 1995a: Passive and active margin history of the northern Tatricum (Western Carpathians, Slovakia). *Geologische Rundschau*, 84, 748–760.

Plašienka, D., 1995b: Mesozoic evolution of Tatric units in the Malé Karpaty and Považský Inovec Mts.: implications for the position of the Klape and related units in Western Slovakia. *Geologica Carpathica*, 46, 2, 101–112.

Plašienka, D., 1996: Cryptic ridges or collision orogenic belts? *Mineralia Slovaca*, 28, 1, 75–79 (in Slovak).

Plašienka, D., 2012a: Jurassic syn-rift and Cretaceous syn-orogenic, coarse-grained deposits related to opening and closure of the Vahic (South Penninic) Ocean in the Western Carpathians – an overview. *Geological Quarterly*, 56, 4, 601–628.

Plašienka, D., 2012b: Early stages of structural evolution of the Carpathian Klippen Belt (Slovakian Pieniny sector). *Mineralia Slovaca*, 44, 1–16.

Plašienka, D., 2018: The Carpathian Klippen Belt and types of its klippen – an attempt at a genetic classification. *Mineralia Slovaca*, 50, 1–24.

Plašienka, D. & Mikuš, V., 2010: Geological setting of the Pieniny and Šariš sectors of the Klippen Belt between Litmanová and Drienica villages in eastern Slovakia. *Mineralia Slovaca*, 42, 2, 155–178 (in Slovak with English Summary).

Plašienka, D. & Soták, J., 2015: Evolution of Late Cretaceous--Palaeogene synorogenic basins in the Pieniny Klippen Belt and adjacent zones (Western Carpathians, Slovakia): Tectonic controls over a growing orogenic wedge. *Annales Societatis Geologorum Poloniae*, 85, 43–76.

Plašienka, D., Soták, J., Jamrichová, M., Halásová, E., Pivko, D., Józsa, Š, Madzin, J. & Mikuš, V., 2012: Structure and evolution of the Pieniny Klippen Belt demonstrated along a section between Jarabina and Litmanová villages in Eastern Slovakia. *Mineralia Slovaca*, 44, 1, 17–39.

Plašienka, D., Józsa, Š, Gedl, P. & Madzin, J., 2013: Fault contact of the Pieniny Klippen Belt with the Central Carpathian Paleogene Basin (Western Carpathians): new data from a unique temporary exposure in Ľutina village (Eastern Slovakia). *Geologica Carpathica*, 64, 165–168.

Plašienka, D., Méres, Š., Ivan, P., Sýkora, M., Soták, J., Lačný, A., Aubrecht, R., Bellová, S. & Potočný, T., 2019: Meliatic blueschists and their detritus in Cretaceous sediments: New data constraining tectonic evolution of the West Carpathians. *Swiss Journal of Geosciences*, 112, 1, 55–81. https://doi.org/10.1007/s00015-018-0330-7.

Plašienka, D., Bučová, J. & Šimonová, V., 2020: Variable structural styles and tectonic evolution of an ancient backstop boundary: the Pieniny Klippen Belt of the Western Carpathians. *International Journal of Earth Sciences*, 109, 4, 1355–1376.

Pober, E. & Faupl, P., 1988: The chemistry of detrital spinels and its application for the geodynamic evolution of the Eastern Alps. *Geologische Rundschau*, 77, 641–670. https://doi.org/10.1007/BF01830175.

Prokešová, R., Plašienka, D. & Milovský, R., 2012: Structural pattern and emplacement mechanisms of the Krížna cover nappe (Western Carpathians, Slovakia). *Geologica Carpathica*, 63, 13–32.

Putiš, M., Scherer, E. E., Nemec, O., Ackerman, L. & Ružička, P., 2023: Geochemistry, Lu–Hf garnet ages, and P–T conditions of blueschists from the Meliatic and Fatric nappes, Western Carpathians: Indicators of Neotethyan subduction. *Geosystems and Geoenvironment*, 2, 100150. https://doi.org/10.1016/j.geogeo.2022.100150.

Rakús, M. & Marschalko, R., 1997: Position of the Manín, Drietoma and Klape units at the boundary of the Central and Outer Carpathians. In: Plašienka, D., Hók, J., Vozár J. & Elečko, M. (eds.): Alpine Evolution of the Western Carpathians and Related areas. International Conference. Abstracts & Introductory Articles to the Excursion. *Bratislava, Geological Survey of Slovak Republic*, 79–97.

Ratschbacher, L., Frisch, W., Linzer, H.-G., Sperner, B., Meschede, M., Decker, K., Nemčok, M., Nemčok, J. & Grygar, R., 1993: The Pieniny Klippen Belt in the Western Carpathians of northeastern Slovakia: structural evidence for transpression. *Tectonophysics*, 226, 471–483. https://doi.org/10.1016/0040-1951(93)90133-5.

Salata, D., 2004: Detrital garnets from the Upper Cretaceous--Palaeogene sandstones of the Polish part of the Magura Nappe and the Pieniny Klippen Belt: chemical constrains. *Annales Societatis Geologorum Poloniae*, 74, 351–364.

Schmid, M. S., Bernoulli, D., Fügenshuh, B., Matenco, L., Schefer, S., Schuster, R., Tichler, M. & Ustaszewski, K., 2008: The Alpine-Carpathian-Dinaridic orogenic system: correlation and evolution of tectonic units. *Swiss Journal of Geosciences*, 101, 139–183. https://doi.org/10.1007/s00015-008-1247-3.

Starek, D., Aubrecht, R., Sliva, Ľ. & Józsa, Š., 2010: Sedimentary analysis of the Cretaceous flysch sequences at the Zemianska Dedina locality (Nižná Unit, Pieniny Klippen Belt, northern Slovakia). *Mineralia Slovaca*, 42, 179–188.

Tomek, Č., 1993: Deep crustal structure beneath the central and inner West Carpathians. Tectonophysics, 226, 417–431. https://doi.org/10.1016/0040-1951(93)90130-C.

Uher, P., Bačík, P. & Ozdín, D., 2009: Tourmaline (magnesiofoitite and dravite) in quartz vein near Limbach, Malé Karpaty Mts. (Slovakia). *Mineralia Slovaca*, 41, 445–456 (in Slovak with English Summary).

Whitney, L. D. & Evans, W. B., 2010: Abbreviations for names of rock-forming minerals. *American Mineralogist*, 95, 185–187. https://doi.org/10.2138/am.2010.3371.

Winkler, Z. & Ślączka, A., 1992: Sediment dispersal and provenance in the Silesian, Dukla and Magura nappes (Outer Carpathians, Poland). *Geologische Rundschau*, 2, 371–382.

Winkler, Z. & Ślączka, A., 1994: A late Cretaceous to Palaeogene geodynamic model for the Western Carpathians in Poland. *Geologica Carpathica*, 45, 2, 71–82.

Analýza ťažkých minerálov vrchnokriedových až spodnoeocénnych synorogenetických sedimentov pieninského bradlového pásma (šarišská jednotka, východné Slovensko): nové údaje z vrtu Jar-2 (jarmutsko-pročské s.) a odkryvov (malinowské s.)

Článok prezentuje nové výsledky analýzy ťažkých minerálov a chemické zloženie detritických granátov, turmalínov a Cr-spinelov z jadrového vrtného materiálu štruktúrneho vrtu Jar-2, ktorý prenikol cez turbiditné pieskovce mástrichtsko-spodnoeocénneho jarmutsko-pročského súvrstvia, a z jemnozrnných pieskovcov hemipelagického turónsko-kampánskeho malinowského súvrstvia (vzorky z odkryvu) šarišskej jednotky pieninského bradlového pásma (PBP) na východnom Slovensku. V asociáciách ťažkých minerálov jarmutsko-pročského súvrstvia dominujú granát, apatit a turmalín. O niečo menej zastúpené sú rutil a zirkón. Sporadicky sa vyskytuje Cr-spinel. V malinowskom súvrství sú dominantné granát a rutil, menej zirkón a turmalín. Cr-spinel sa vyskytuje častejšie, pričom najmenej zastúpený ťažký minerál je tu apatit.

V oboch súvrstviach dominujú almandínové granáty s rôznym pomerom grosuláru, pyropu a spessartínu. Analyzované granáty boli derivované prevažne z nízko-, stredno- až vysokostupňových polymetamorfovaných komplexov. O niečo pestrejšia populácia granátov v jarmutsko-pročskom súvrství môže odrážať nový prínos granátov zo stredne metamorfovaných bázickejších zdrojov počas najvrchnejšej kriedy. Niektoré z almandínových granátov môžu pochádzať aj z granitoidných hornín. Časť analyzovaných almandínových granátov s nízkym obsahom pyropu, vyšším obsahom grosulárovej molekuly a variabilným obsahom spessartínu je podobná granátom z obliakov metabazitov v albsko-cenomanských zlepencoch klapskej jednotky a vysokotlakovo a nízkoteplotne metamorfovaného príkrovu Bôrky (Putiš et al., 2023). Môže to indikovať ich pôvod v meliatiku.

Analyzované detritické turmalíny vykazujú zložitú optickú zonalitu. Na základe bodových analýz z odlišných optických zón najčastejším typom turmalínov sú X-vakantné turmalíny. Menej časté sú alkalické turmalíny a zriedkavo zastúpené sú vápenaté turmalíny. X-vakantné turmalíny majú stredný obsah vakancií a zložením zodpovedajú magneziofoititu až foititu. Alkalické turmalíny chemickým zložením zodpovedajú skorylu-dravitu. Vápenaté turmalíny zodpovedajú uvitu a feruvitu. Magneziofoitity až foitity tvoria buď jadrá zŕn, oscilačné zóny, alebo opticky zložité zóny a okraje zŕn. Niektoré zrná alebo zóny so skorylovo-dravitovým zložením sú charakteristické jemným prerastaním s kremeňom a početnými minerálnymi inklúziami. Minerálne inklúzie tvoria kremeň, rutil, zirkón, monazit, titanit, ilmenit, apatit, allanit, albit a oxidy železa. Významný obsah podobných komplexne zonálnych detritických turmalínov bol nedávno objavený v kriedových súvrstviach s „exotickými“ zlepencami z centrálnych Západných Karpát (CZK) a PBP (Bellová et al., 2018; Plašienka et al., 2019; Aubrecht et al., 2020a, 2020b, 2021). Komplexne zonálne turmalíny môžu pochádzať z exhumovaných vysokotlakovo-nízkoteplotných ofiolitových komplexov meliatika (l. c.). Zdanlivý paradox ich výskytu vo flyšových súvrstviach uložených na opačnej (externej) strane orogénneho pásma a ich derivácia z „južných“ (interných) západokarpatských zón sa dá vysvetliť viacfázovou recykláciou, ako sa predpokladá aj pri derivácii ofiolitového detritu s harzburgitovým zložením v kriedových až paleogénnych flyšových súvrstviach CZK a PBP (Plašienka, 2012a a tamojšie citácie). Ofiolitové komplexy meliatika boli počas spodnej kriedy vystavené erózii v interných západokarpatských zónach. Ofiolitový detrit a „exotický“ obliakový materiál bol uložený najprv vo flyšových sedimentoch albsko-cenomanského porubského súvrstvia v zliechovskej panve fatrika. Porubské súvrstvie ako súčasť príkrovového systému fatrika bolo počas vrchného turónu presunuté do pozície falošného akrečného klina za tatrickým externým okrajom. Tam sa stalo súčasťou klapskej jednotky pribradlovej zóny (Plašienka, 1995a, 1995b, 1996, 2012a; Prokešová et al., 2012; Plašienka et al., 2019). Albsko-cenomanské flyšové súvrstvia klapskej jednotky, už kompletne zahrnuté do rastúceho akrečného klina, mohli takýmto spôsobom tvoriť „proximálny“ zdroj ofiolitového detritu aj komplexne zonálnych turmalínov pre čoraz mladšie synorogenetické súvrstvia v čelných panvách PBP a priľahlých zón (Plašienka, 2012a; Plašienka & Soták, 2015; Plašienka et al., 2019; Madzin & Plašienka, 2022).

Analyzované Cr-spinely nevykazujú žiadne znaky premeny alebo zonality. Takmer všetky študované Cr-spinely oboch súvrství majú pomer Fe^{2+}/Fe^{3+} vyšší ako 4, čo je charakteristické pre spinely plášťových peridotitov (Lenaz et al., 2000; Kamenetsky et al., 2001). Analyzované Cr-spinely najlepšie zodpovedajú harzburgitom alebo podiformným chromititom (Pober & Faupl, 1988). Iba niekoľko Cr-spinelov z malinowského súvrstvia vykazuje koncentráciu TiO_2 vyššiu ako 0,2 hm. %, čo naznačuje ich pôvod vo vulkanických horninách. Vulkanické spinely svojím zložením zodpovedajú bazaltom vulkanických

oblúkov alebo zaoblúkových paniev (Lenaz et al., 2000; Kamenetsky et al., 2001).

Zdroj ofiolitového detritu vo vrchnokriedových klastických súvrstviach PBP sa všeobecne považuje za rovnaký ako zdroj „exotických" zlepencov klapskej jednotky. Hoci pôvod, paleogeografická pozícia a interpretácia klapskej jednotky sú predmetom desaťročia trvajúcej diskusie, v poslednom čase panuje konsenzus, že ofiolitový detrit pochádza z ofiolitových komplexov meliatika v interných západokarpatských zónach (Aubrecht et al., 2009; Plašienka, 2012a; Bellová et al., 2018; Plašienka et al., 2019; Aubrecht et al., 2020a, 2020b, 2021; Putiš et al., 2023). Chemické zloženie Cr-spinelov a komplexne zonálnych turmalínov analyzovaných v tejto práci túto predstavu podporuje. Vysoký verzus nízky obsah Cr-spinelov v proximálnych verzus distálnych turónsko-kampánskych sedimentoch pieninskej a šarišskej jednotky a smerom nahor sa znižujúci obsah Cr-spinelov vo vrchnokriedových až spodnoeocénnych flyšových sedimentoch PBP je v súlade s konceptom viacnásobnej recyklácie ofiolitového detritu z klapskej jednotky.

Doručené / Recieved: 31. 12. 2025
Prijaté na publikovanie / Accepted: 10. 3. 2026

Supplementary Table S1

Representative microprobe analyses of detrital garnets from Upper Cretaceous to Paleocene deposits of the Jarmuta-Proč Fm., structural drill JAR-2, Pieniny sector of the PKB, Western Carpathians, Slovakia

Locality	Jarabina JAR-2	Jarabina JAR-2	Jarabina JAR-2	Jarabina JAR-2	Jarabina JAR-2	Jarabina JAR-2	Jarabina JAR-2	Jarabina JAR-2	Jarabina JAR-2	Jarabina JAR-2	Jarabina JAR-2	Jarabina JAR-2	Jarabina JAR-2	Jarabina JAR-2
Formation	Jarmuta-Proč Fm.	Jarmuta-Proč Fm.	Jarmuta-Proč Fm.	Jarmuta-Proč Fm.	Jarmuta-Proč Fm.	Jarmuta-Proč Fm.	Jarmuta-Proč Fm.	Jarmuta-Proč Fm.	Jarmuta-Proč Fm.	Jarmuta-Proč Fm.	Jarmuta-Proč Fm.	Jarmuta-Proč Fm.	Jarmuta-Proč Fm.	Jarmuta-Proč Fm.
Age	Maastrichtian–Middle Eocene	Maastrichtian–Middle Eocene	Maastrichtian–Middle Eocene	Maastrichtian–Middle Eocene	Maastrichtian–Middle Eocene	Maastrichtian–Middle Eocene	Maastrichtian–Middle Eocene	Maastrichtian–Middle Eocene	Maastrichtian–Middle Eocene	Maastrichtian–Middle Eocene	Maastrichtian–Middle Eocene	Maastrichtian–Middle Eocene	Maastrichtian–Middle Eocene	Maastrichtian–Middle Eocene
Unit	Šariš U.	Šariš U.	Šariš U.	Šariš U.	Šariš U.	Šariš U.	Šariš U.	Šariš U.	Šariš U.	Šariš U.	Šariš U.	Šariš U.	Šariš U.	Šariš U.
Sample	JAR-2A	JAR-2A	JAR-2A	JAR-2A	JAR-2A	JAR-2A	JAR-2A	JAR-2A	JAR-2A	JAR-2A	JAR-2A	JAR-2A	JAR-2A	JAR-2A
Point	an5	an8	an14	an15	an16	an17	an18	an19	an20	an21	an22	an23	an24	an25
SiO_2	37.21	37.26	37.44	37.50	36.89	38.36	37.72	36.91	37.01	37.11	37.30	37.86	37.25	37.59
TiO_2	0.04	0.18	0.02	0.00	0.06	0.02	0.01	0.04	0.10	0.00	0.09	0.06	0.11	0.06
Al_2O_3	21.32	21.25	21.07	21.59	21.35	22.03	21.05	20.97	21.18	21.05	21.06	21.74	21.08	21.35
Cr_2O_3	0.03	0.02	0.00	0.00	0.00	0.02	0.00	0.00	0.00	0.04	0.00	0.04	0.04	0.00
$Fe_2O_3^*$	0.00	0.00	0.00	0.00	0.00	0.00	0.00	0.07	0.00	0.10	0.00	0.00	0.00	0.00
FeO	34.08	28.25	35.66	32.70	36.87	31.30	33.39	33.75	31.51	33.37	35.39	30.07	34.23	34.35
MnO	1.25	6.00	0.47	2.39	0.74	0.71	2.50	2.13	3.09	4.70	0.56	0.72	0.99	1.04
MgO	3.33	1.13	2.82	2.61	2.70	6.43	3.10	0.27	1.24	2.36	1.76	4.60	1.27	4.63
NiO	0.00	0.00	0.00	0.00	0.00	0.00	0.00	0.00	0.00	0.00	0.00	0.00	0.00	0.00
ZnO	0.00	0.00	0.00	0.00	0.00	0.00	0.00	0.00	0.00	0.00	0.00	0.00	0.00	0.00
CaO	2.13	6.39	2.16	3.94	1.57	1.48	2.25	6.22	5.81	1.78	3.64	5.01	4.67	0.94
Total	99.38	100.47	99.64	100.72	100.17	100.35	100.02	100.34	99.93	100.51	99.79	100.10	99.63	99.96
Formulae based on 12 oxygens and with Fe^{2+}/Fe^{3+} calculated assuming full occupancy														
Si	2.99	2.99	3.01	2.98	2.97	2.99	3.02	2.99	2.99	2.99	3.01	2.98	3.00	2.99
Al iv	0.01	0.01	0.00	0.02	0.03	0.01	0.00	0.01	0.01	0.01	0.00	0.02	0.00	0.01
Al vi	2.01	1.99	2.00	2.01	2.00	2.02	1.99	1.99	2.00	1.99	2.01	2.00	2.01	2.00
Ti	0.00	0.01	0.00	0.00	0.00	0.00	0.00	0.00	0.01	0.00	0.01	0.00	0.01	0.00
Cr	0.00	0.00	0.00	0.00	0.00	0.00	0.00	0.00	0.00	0.00	0.00	0.00	0.00	0.00
Fe^{3+}	0.00	0.00	0.00	0.00	0.00	0.00	0.00	0.00	0.00	0.01	0.00	0.00	0.00	0.00
Fe^{2+}	2.32	1.90	2.42	2.19	2.49	2.07	2.25	2.29	2.13	2.25	2.41	1.99	2.34	2.30
Mn	0.08	0.41	0.03	0.16	0.05	0.05	0.17	0.15	0.21	0.32	0.04	0.05	0.07	0.07
Mg	0.40	0.14	0.34	0.31	0.32	0.75	0.37	0.03	0.15	0.28	0.21	0.54	0.15	0.55
Ni	0.00	0.00	0.00	0.00	0.00	0.00	0.00	0.00	0.00	0.00	0.00	0.00	0.00	0.00
Zn	0.00	0.00	0.00	0.00	0.00	0.00	0.00	0.00	0.00	0.00	0.00	0.00	0.00	0.00
Ca	0.18	0.55	0.19	0.34	0.14	0.12	0.19	0.54	0.50	0.15	0.31	0.42	0.40	0.08
Total	8.00	8.00	7.99	8.01	8.01	8.00	7.99	8.00	8.00	8.01	7.99	8.01	7.99	8.00
End members														
Almandine	77.65	63.44	81.29	72.97	82.85	69.27	75.40	75.97	71.14	74.66	81.03	66.08	78.97	76.62
Andradite	0.00	0.00	0.00	0.00	0.00	0.00	0.00	0.21	0.00	0.31	0.00	0.00	0.00	0.00
Grossular	6.06	18.33	6.26	11.26	4.55	4.06	6.48	17.84	16.81	4.71	10.57	14.04	13.50	2.69
Pyrope	13.36	4.53	11.38	10.37	10.89	25.04	12.42	1.08	4.97	9.47	7.10	18.13	5.14	18.36
Spessartine	2.84	13.65	1.08	5.40	1.71	1.56	5.69	4.90	7.07	10.72	1.30	1.61	2.28	2.34
Uvarovite	0.09	0.06	0.00	0.00	0.00	0.07	0.00	0.00	0.00	0.12	0.00	0.14	0.12	0.00
% cations	99.45	99.55	99.36	99.39	99.00	99.44	99.49	99.62	99.49	99.61	99.27	99.31	99.05	99.84
*calculated														

Supplementary Table S1 – continuation

Locality	Jarabina JAR-2	Jarabina JAR-2	Jarabina JAR-2	Jarabina JAR-2	Jarabina JAR-2	Jarabina JAR-2	Jarabina JAR-2	Jarabina JAR-2	Jarabina JAR-2	Jarabina JAR-2	Jarabina JAR-2	Jarabina JAR-2	Jarabina JAR-2	Jarabina JAR-2
Formation	Jarmuta-Proč Fm.	Jarmuta-Proč Fm.	Jarmuta-Proč Fm.	Jarmuta-Proč Fm.	Jarmuta-Proč Fm.	Jarmuta-Proč Fm.	Jarmuta-Proč Fm.	Jarmuta-Proč Fm.	Jarmuta-Proč Fm.	Jarmuta-Proč Fm.	Jarmuta-Proč Fm.	Jarmuta-Proč Fm.	Jarmuta-Proč Fm.	Jarmuta-Proč Fm.
Age	Maastrichtian–Middle Eocene	Maastrichtian–Middle Eocene	Maastrichtian–Middle Eocene	Maastrichtian–Middle Eocene	Maastrichtian–Middle Eocene	Maastrichtian–Middle Eocene	Maastrichtian–Middle Eocene	Maastrichtian–Middle Eocene	Maastrichtian–Middle Eocene	Maastrichtian–Middle Eocene	Maastrichtian–Middle Eocene	Maastrichtian–Middle Eocene	Maastrichtian–Middle Eocene	Maastrichtian–Middle Eocene
Unit	Šariš U.	Šariš U.	Šariš U.	Šariš U.	Šariš U.	Šariš U.	Šariš U.	Šariš U.	Šariš U.	Šariš U.	Šariš U.	Šariš U.	Šariš U.	Šariš U.
Sample	JAR-2A	JAR-2A	JAR-2A	JAR-2A	JAR-2B	JAR-2B	JAR-2B	JAR-2B	JAR-2B	JAR-2B	JAR-2B	JAR-2B	JAR-2B	JAR-2B
Point	an26	an27	an28	an29	an1	an2	an3	an6	an7	an13	an14	an15	an16	an17
SiO_2	36.98	37.24	37.62	37.14	37.25	37.32	37.09	36.86	37.19	37.08	37.46	37.88	36.90	37.39
TiO_2	0.02	0.04	0.07	0.06	0.07	0.06	0.00	0.06	0.00	0.06	0.04	0.06	0.11	0.08
Al_2O_3	21.25	21.02	21.30	21.13	21.15	21.29	21.17	20.82	21.07	20.90	21.72	21.42	20.34	20.91
Cr_2O_3	0.01	0.01	0.01	0.03	0.05	0.02	0.01	0.02	0.00	0.00	0.00	0.03	0.04	0.00
Fe_2O_3*	0.00	0.00	0.00	0.00	0.00	0.00	0.00	0.00	0.00	0.08	0.00	0.00	0.46	0.09
FeO	35.46	34.62	34.44	33.64	31.82	34.57	33.01	31.78	31.72	25.70	34.13	24.96	19.48	30.23
MnO	2.01	1.27	0.15	5.02	3.14	1.02	5.60	2.48	6.08	10.15	1.24	3.01	17.15	3.08
MgO	1.96	1.36	3.23	1.63	2.24	3.88	2.69	0.66	2.40	0.87	4.04	2.42	1.49	2.72
NiO	0.00	0.00	0.00	0.00	0.00	0.00	0.00	0.00	0.00	0.00	0.00	0.00	0.00	0.00
ZnO	0.00	0.00	0.00	0.00	0.00	0.00	0.00	0.00	0.00	0.00	0.00	0.00	0.00	0.00
CaO	2.39	4.39	3.37	1.59	3.65	1.34	0.69	6.54	1.36	5.34	1.85	9.35	3.59	4.96
Total	100.08	99.94	100.19	100.24	99.36	99.50	100.25	99.22	99.82	100.18	100.48	99.13	99.55	99.45
Formulae based on 12 oxygens and with Fe^{2+}/Fe^{3+} calculated assuming full occupancy														
Si	2.99	3.01	3.00	3.00	3.00	2.99	2.99	3.00	3.00	3.00	2.97	3.01	3.00	3.01
Al iv	0.01	0.00	0.00	0.00	0.00	0.01	0.01	0.00	0.00	0.00	0.03	0.00	0.00	0.00
Al vi	2.01	2.00	2.00	2.01	2.01	2.01	2.00	2.00	2.01	1.99	2.01	2.01	1.95	1.98
Ti	0.00	0.00	0.00	0.00	0.00	0.00	0.00	0.00	0.00	0.00	0.00	0.00	0.01	0.00
Cr	0.00	0.00	0.00	0.00	0.00	0.00	0.00	0.00	0.00	0.00	0.00	0.00	0.00	0.00
Fe^{3+}	0.00	0.00	0.00	0.00	0.00	0.00	0.00	0.00	0.00	0.00	0.00	0.00	0.03	0.01
Fe^{2+}	2.41	2.35	2.31	2.30	2.17	2.34	2.23	2.17	2.16	1.74	2.28	1.69	1.33	2.03
Mn	0.14	0.09	0.01	0.34	0.21	0.07	0.38	0.17	0.42	0.70	0.08	0.20	1.18	0.21
Mg	0.24	0.16	0.38	0.20	0.27	0.46	0.32	0.08	0.29	0.10	0.48	0.29	0.18	0.33
Ni	0.00	0.00	0.00	0.00	0.00	0.00	0.00	0.00	0.00	0.00	0.00	0.00	0.00	0.00
Zn	0.00	0.00	0.00	0.00	0.00	0.00	0.00	0.00	0.00	0.00	0.00	0.00	0.00	0.00
Ca	0.21	0.38	0.29	0.14	0.32	0.12	0.06	0.57	0.12	0.46	0.16	0.80	0.31	0.43
Total	8.00	7.99	8.00	8.00	7.99	8.00	8.00	8.00	8.00	8.00	8.01	7.99	8.00	8.00
End members														
Almandine	80.59	78.88	77.18	77.24	73.14	78.28	74.40	72.53	72.41	57.86	75.83	56.74	43.64	67.69
Andradite	0.00	0.00	0.00	0.00	0.00	0.00	0.00	0.00	0.00	0.24	0.00	0.00	1.42	0.27
Grossular	6.87	12.72	9.60	4.53	10.47	3.82	1.95	19.01	3.95	15.19	5.30	26.71	8.99	14.08
Pyrope	7.89	5.47	12.84	6.60	9.05	15.52	10.83	2.68	9.70	3.50	16.07	9.66	6.07	10.93
Spessartine	4.61	2.91	0.34	11.55	7.20	2.33	12.79	5.72	13.94	23.20	2.81	6.82	39.76	7.03
Uvarovite	0.04	0.02	0.04	0.09	0.15	0.05	0.03	0.06	0.00	0.01	0.00	0.08	0.13	0.00
% cations	99.50	99.52	99.70	99.29	99.20	99.56	99.66	99.79	99.52	99.87	99.02	99.17	99.19	99.44
*calculated														

Supplementary Table S1 – continuation

Locality	Jarabina JAR-2	Jarabina JAR-2	Jarabina JAR-2	Jarabina JAR-2	Jarabina JAR-2	Jarabina JAR-2	Jarabina JAR-2	Jarabina JAR-2	Jarabina JAR-2	Jarabina JAR-2	Jarabina JAR-2	Jarabina JAR-2	Jarabina JAR-2	Jarabina JAR-2
Formation	Jarmuta-Proč Fm.	Jarmuta-Proč Fm.	Jarmuta-Proč Fm.	Jarmuta-Proč Fm.	Jarmuta-Proč Fm.	Jarmuta-Proč Fm.	Jarmuta-Proč Fm.	Jarmuta-Proč Fm.	Jarmuta-Proč Fm.	Jarmuta-Proč Fm.	Jarmuta-Proč Fm.	Jarmuta-Proč Fm.	Jarmuta-Proč Fm.	Jarmuta-Proč Fm.
Age	Maastrichtian–Middle Eocene	Maastrichtian–Middle Eocene	Maastrichtian–Middle Eocene	Maastrichtian–Middle Eocene	Maastrichtian–Middle Eocene	Maastrichtian–Middle Eocene	Maastrichtian–Middle Eocene	Maastrichtian–Middle Eocene	Maastrichtian–Middle Eocene	Maastrichtian–Middle Eocene	Maastrichtian–Middle Eocene	Maastrichtian–Middle Eocene	Maastrichtian–Middle Eocene	Maastrichtian–Middle Eocene
Unit	Šariš U.	Šariš U.	Šariš U.	Šariš U.	Šariš U.	Šariš U.	Šariš U.	Šariš U.	Šariš U.	Šariš U.	Šariš U.	Šariš U.	Šariš U.	Šariš U.
Sample	JAR-2B	JAR-2B	JAR-2B	JAR-2C	JAR-2C	JAR-2C	JAR-2C	JAR-2C	JAR-2C	JAR-2C	JAR-2C	JAR-2C	JAR-2C	JAR-2C
Point	an19	an21	an29	an2	an4	an5	an6	an9	an10	an16	an17	an19	an20	an21
SiO_2	36.83	37.20	37.84	37.40	37.84	37.26	37.63	37.77	37.38	37.72	37.92	37.62	37.88	38.45
TiO_2	0.00	0.00	0.11	0.05	0.13	0.04	0.02	0.09	0.05	0.03	0.03	0.04	0.06	0.04
Al_2O_3	21.29	21.39	21.41	21.28	21.40	21.03	21.43	21.33	21.18	21.50	21.46	21.55	21.57	21.60
Cr_2O_3	0.00	0.00	0.05	0.01	0.00	0.02	0.00	0.00	0.02	0.03	0.00	0.03	0.03	0.00
$Fe_2O_3^*$	0.00	0.00	0.00	0.00	0.00	0.00	0.00	0.00	0.00	0.00	0.00	0.00	0.00	0.00
FeO	33.57	35.36	24.77	32.96	27.03	36.52	33.03	28.88	34.46	34.96	31.80	31.61	30.42	31.75
MnO	4.46	0.73	4.57	3.90	3.59	0.64	3.84	0.57	3.62	1.29	0.45	0.68	0.51	0.73
MgO	2.32	3.18	1.20	0.97	1.25	1.35	2.99	1.18	2.72	3.67	4.37	2.02	1.56	5.05
NiO	0.00	0.00	0.00	0.00	0.00	0.00	0.00	0.00	0.00	0.00	0.00	0.00	0.00	0.00
ZnO	0.00	0.00	0.00	0.00	0.00	0.00	0.00	0.00	0.00	0.00	0.00	0.00	0.00	0.00
CaO	1.35	1.89	10.69	4.10	9.60	3.05	1.42	9.98	1.02	1.06	3.70	6.76	8.82	2.73
Total	99.82	99.75	100.66	100.67	100.84	99.90	100.35	99.80	100.45	100.25	99.73	100.31	100.85	100.35
Formulae based on 12 oxygens and with Fe^{2+}/Fe^{3+} calculated assuming full occupancy														
Si	2.98	2.99	2.99	3.00	3.00	3.01	3.00	3.01	3.00	3.00	3.00	2.99	2.99	3.01
Al iv	0.02	0.01	0.01	0.00	0.00	0.00	0.00	0.00	0.00	0.00	0.00	0.01	0.01	0.00
Al vi	2.01	2.02	1.99	2.02	1.99	2.01	2.02	2.01	2.01	2.02	2.01	2.01	2.00	2.00
Ti	0.00	0.00	0.01	0.00	0.01	0.00	0.00	0.01	0.00	0.00	0.00	0.00	0.00	0.00
Cr	0.00	0.00	0.00	0.00	0.00	0.00	0.00	0.00	0.00	0.00	0.00	0.00	0.00	0.00
Fe^{3+}	0.00	0.00	0.00	0.00	0.00	0.00	0.00	0.00	0.00	0.00	0.00	0.00	0.00	0.00
Fe^{2+}	2.29	2.40	1.64	2.24	1.79	2.50	2.23	1.94	2.33	2.36	2.12	2.12	2.02	2.10
Mn	0.31	0.05	0.31	0.26	0.24	0.04	0.26	0.04	0.25	0.09	0.03	0.05	0.03	0.05
Mg	0.28	0.38	0.14	0.12	0.15	0.16	0.36	0.14	0.33	0.43	0.52	0.24	0.18	0.59
Ni	0.00	0.00	0.00	0.00	0.00	0.00	0.00	0.00	0.00	0.00	0.00	0.00	0.00	0.00
Zn	0.00	0.00	0.00	0.00	0.00	0.00	0.00	0.00	0.00	0.00	0.00	0.00	0.00	0.00
Ca	0.12	0.16	0.91	0.35	0.81	0.26	0.12	0.85	0.09	0.09	0.31	0.58	0.75	0.23
Total	8.01	8.00	8.00	7.99	8.00	7.99	7.99	7.99	8.00	8.00	8.00	8.00	8.00	7.99
End members														
Almandine	76.43	80.15	54.76	75.33	59.84	84.18	75.23	65.39	77.93	79.39	71.16	71.17	67.73	70.79
Andradite	0.00	0.00	0.00	0.00	0.00	0.00	0.00	0.00	0.00	0.00	0.00	0.00	0.00	0.00
Grossular	3.92	5.43	30.13	11.81	27.18	8.83	4.08	28.60	2.88	2.96	10.52	19.20	24.89	7.71
Pyrope	9.41	12.74	4.73	3.92	4.93	5.46	11.96	4.71	10.89	14.64	17.30	8.00	6.16	19.85
Spessartine	10.25	1.66	10.24	8.91	8.04	1.46	8.73	1.29	8.24	2.92	1.01	1.54	1.14	1.64
Uvarovite	0.00	0.01	0.15	0.04	0.00	0.07	0.00	0.00	0.06	0.08	0.01	0.09	0.08	0.01
% cations	99.29	99.57	99.84	99.24	99.89	99.10	99.17	99.30	99.61	99.14	99.53	99.51	99.67	99.26
*calculated														

Supplementary Table S1 – continuation

Locality	Jarabina JAR-2	Jarabina JAR-2	Jarabina JAR-2	Ľutina	Ľutina	Ľutina	Ľutina	Ľutina	Ľutina	Ľutina	Ľutina	Ľutina	Ľutina	Ľutina
Formation	Jarmuta-Proč Fm.	Jarmuta-Proč Fm.	Jarmuta-Proč Fm.	Malinowa Fm.	Malinowa Fm.	Malinowa Fm.	Malinowa Fm.	Malinowa Fm.	Malinowa Fm.	Malinowa Fm.	Malinowa Fm.	Malinowa Fm.	Malinowa Fm.	Malinowa Fm.
Age	Maastrichtian–Middle Eocene	Maastrichtian–Middle Eocene	Maastrichtian–Middle Eocene	Turonian–Campanian	Turonian–Campanian	Turonian–Campanian	Turonian–Campanian	Turonian–Campanian	Turonian–Campanian	Turonian–Campanian	Turonian–Campanian	Turonian–Campanian	Turonian–Campanian	Turonian–Campanian
Unit	Šariš U.	Šariš U.	Šariš U.	Šariš U.	Šariš U.	Šariš U.	Šariš U.	Šariš U.	Šariš U.	Šariš U.	Šariš U.	Šariš U.	Šariš U.	Šariš U.
Sample	JAR-2C	JAR-2C	JAR-2C	LU-5A	LU-5A	LU-5A	LU-5A	LU-5A	LU-5A	LU-5A	LU-5A	LU-5A	LU-5A	LU-5A
Point	an22	an23	an24	an12	an14	an22	an23	an24	an31	an32	an33	an39	an40	an41
SiO_2	36.98	38.13	37.57	37.82	38.81	37.57	36.80	37.52	36.57	37.16	37.20	37.61	37.33	37.54
TiO_2	0.03	0.04	0.10	0.01	0.05	0.03	0.00	0.02	0.00	0.06	0.05	0.00	0.00	0.02
Al_2O_3	20.98	21.74	21.09	21.56	22.29	21.30	21.12	21.51	21.04	21.01	21.13	21.19	21.00	21.35
Cr_2O_3	0.01	0.10	0.02	0.01	0.05	0.01	0.03	0.00	0.02	0.00	0.04	0.04	0.04	0.01
$Fe_2O_3^*$	0.24	0.00	0.00	0.00	0.00	0.00	0.00	0.00	0.00	0.20	0.00	0.00	0.00	0.00
FeO	37.54	31.48	31.88	31.31	27.16	33.17	29.70	33.28	31.06	33.15	35.69	32.11	34.07	32.39
MnO	1.31	1.87	2.81	5.96	0.34	1.61	8.39	1.96	9.26	4.05	1.38	2.45	1.75	0.97
MgO	1.71	5.37	0.95	3.00	7.23	3.59	2.28	3.90	1.48	2.65	2.82	3.50	3.18	3.60
NiO	0.00	0.00	0.00	0.00	0.00	0.00	0.00	0.00	0.00	0.00	0.00	0.00	0.00	0.00
ZnO	0.00	0.00	0.00	0.00	0.00	0.00	0.00	0.00	0.00	0.00	0.00	0.00	0.00	0.00
CaO	2.11	1.45	6.06	1.58	4.36	2.57	1.05	1.40	0.30	2.13	1.39	2.74	2.31	3.51
Total	100.90	100.17	100.48	101.25	100.29	99.84	99.36	99.59	99.71	100.41	99.70	99.63	99.67	99.39
Formulae based on 12 oxygens and with Fe^{2+}/Fe^{3+} calculated assuming full occupancy														
Si	2.98	3.00	3.01	3.00	2.99	3.00	2.99	2.99	2.99	2.99	3.00	3.01	3.01	3.00
Al iv	0.02	0.00	0.00	0.00	0.01	0.00	0.01	0.01	0.01	0.01	0.00	0.00	0.00	0.00
Al vi	1.98	2.01	1.99	2.01	2.01	2.01	2.02	2.02	2.01	1.98	2.01	2.00	1.99	2.01
Ti	0.00	0.00	0.01	0.00	0.00	0.00	0.00	0.00	0.00	0.00	0.00	0.00	0.00	0.00
Cr	0.00	0.01	0.00	0.00	0.00	0.00	0.00	0.00	0.00	0.00	0.00	0.00	0.00	0.00
Fe^{3+}	0.01	0.00	0.00	0.00	0.00	0.00	0.00	0.00	0.00	0.01	0.00	0.00	0.00	0.00
Fe^{2+}	2.53	2.10	2.15	2.09	1.77	2.23	2.04	2.26	2.14	2.23	2.43	2.16	2.30	2.19
Mn	0.09	0.12	0.19	0.40	0.02	0.11	0.58	0.13	0.64	0.28	0.09	0.17	0.12	0.07
Mg	0.21	0.63	0.11	0.35	0.83	0.43	0.28	0.46	0.18	0.32	0.34	0.42	0.38	0.43
Ni	0.00	0.00	0.00	0.00	0.00	0.00	0.00	0.00	0.00	0.00	0.00	0.00	0.00	0.00
Zn	0.00	0.00	0.00	0.00	0.00	0.00	0.00	0.00	0.00	0.00	0.00	0.00	0.00	0.00
Ca	0.18	0.12	0.52	0.13	0.36	0.22	0.09	0.12	0.03	0.18	0.12	0.24	0.20	0.30
Total	8.01	8.00	7.99	8.00	8.00	8.00	8.00	8.00	8.00	8.01	8.00	7.99	8.00	8.00
End members														
Almandine	84.00	70.56	72.33	70.21	59.39	74.68	68.36	75.90	71.65	74.01	81.42	72.57	76.63	73.33
Andradite	0.74	0.00	0.00	0.00	0.00	0.00	0.00	0.00	0.00	0.60	0.00	0.00	0.00	0.00
Grossular	5.35	3.77	17.39	4.48	11.92	7.32	2.96	4.03	0.82	5.53	3.91	7.78	6.53	10.06
Pyrope	6.90	21.16	3.79	11.87	27.81	14.31	9.25	15.61	6.04	10.62	11.38	13.98	12.74	14.38
Spessartine	2.99	4.19	6.41	13.41	0.74	3.65	19.33	4.45	21.44	9.24	3.17	5.56	3.99	2.20
Uvarovite	0.02	0.33	0.07	0.02	0.14	0.04	0.09	0.00	0.05	0.00	0.12	0.11	0.12	0.03
% cations	99.37	99.24	99.39	99.51	99.49	99.60	99.52	99.16	99.53	99.60	99.44	99.50	99.81	99.44
*calculated														

Supplementary Table S1 – continuation

Locality	Ľutina	Ľutina	Ľutina	Ľutina	Ľutina	Ľutina	Ľutina	Ľutina	Ľutina	Ľutina	Ľutina	Ľutina	Ľutina	Ľutina	Ľutina	Ľutina
Formation	Malinowa Fm.	Malinowa Fm.	Malinowa Fm.	Malinowa Fm.	Malinowa Fm.	Malinowa Fm.	Malinowa Fm.	Malinowa Fm.	Malinowa Fm.	Malinowa Fm.	Malinowa Fm.	Malinowa Fm.	Malinowa Fm.	Malinowa Fm.	Malinowa Fm.	Malinowa Fm.
Age	Turonian–Campanian	Turonian–Campanian	Turonian–Campanian	Turonian–Campanian	Turonian–Campanian	Turonian–Campanian	Turonian–Campanian	Turonian–Campanian	Turonian–Campanian	Turonian–Campanian	Turonian–Campanian	Turonian–Campanian	Turonian–Campanian	Turonian–Campanian	Turonian–Campanian	Turonian–Campanian
Unit	Šariš U.	Šariš U.	Šariš U.	Šariš U.	Šariš U.	Šariš U.	Šariš U.	Šariš U.	Šariš U.	Šariš U.	Šariš U.	Šariš U.	Šariš U.	Šariš U.	Šariš U.	Šariš U.
Sample	LU-5A	LU-5A	LU-5A	LU-5B	LU-5B	LU-5B	LU-5B	LU-5B	LU-5B	LU-5B	LU-5B	LU-5B	LU-5B	LU-5B	LU-5B	LU-5B
Point	an43	an44	an52	an1	an2	an3	an4	an5	an8	an9	an10	an11	an13	an17	an19	an21
SiO_2	37.81	37.30	36.34	38.00	37.31	37.58	38.01	37.77	37.50	37.64	38.08	37.81	37.80	37.68	37.77	37.76
TiO_2	0.05	0.01	0.10	0.08	0.00	0.00	0.01	0.00	0.00	0.00	0.00	0.01	0.06	0.02	0.12	0.03
Al_2O_3	21.68	21.30	20.87	21.55	21.26	21.58	21.25	21.40	21.45	21.40	21.82	21.51	21.37	21.53	21.27	21.34
Cr_2O_3	0.02	0.00	0.00	0.00	0.02	0.03	0.00	0.01	0.02	0.02	0.01	0.01	0.04	0.00	0.00	0.00
$Fe_2O_3^*$	0.00	0.00	0.00	0.00	0.00	0.00	0.00	0.00	0.00	0.00	0.00	0.00	0.15	0.00	0.00	0.43
FeO	31.92	31.53	28.83	31.22	34.81	32.94	33.85	32.53	33.39	34.01	32.35	31.45	31.17	34.26	25.36	19.23
MnO	1.71	3.16	10.78	0.89	2.93	1.17	0.47	2.26	1.97	1.78	0.77	1.10	0.68	2.03	5.31	17.20
MgO	4.16	3.31	1.61	4.57	2.67	3.68	4.08	3.42	3.51	3.81	4.56	4.65	4.55	3.61	1.26	3.63
NiO	0.00	0.00	0.00	0.00	0.00	0.00	0.00	0.00	0.00	0.00	0.00	0.00	0.00	0.00	0.00	0.00
ZnO	0.00	0.00	0.00	0.00	0.00	0.00	0.00	0.00	0.00	0.00	0.00	0.00	0.00	0.00	0.00	0.00
CaO	2.91	2.49	0.73	3.23	0.92	3.11	2.40	2.30	2.34	1.39	3.07	3.23	4.27	1.63	9.15	2.00
Total	100.26	99.10	99.26	99.54	99.92	100.09	100.07	99.69	100.19	100.05	100.66	99.78	100.10	100.76	100.24	101.61
Formulae based on 12 oxygens and with Fe^{2+}/Fe^{3+} calculated assuming full occupancy																
Si	2.99	3.00	2.98	3.00	3.00	2.99	3.02	3.01	2.99	3.00	2.99	3.00	2.99	2.99	3.00	2.98
Al iv	0.01	0.00	0.02	0.00	0.00	0.01	0.00	0.00	0.01	0.00	0.01	0.00	0.01	0.01	0.00	0.02
Al vi	2.01	2.02	2.00	2.01	2.02	2.01	1.99	2.02	2.01	2.01	2.01	2.01	1.98	2.01	2.00	1.97
Ti	0.00	0.00	0.01	0.00	0.00	0.00	0.00	0.00	0.00	0.00	0.00	0.00	0.00	0.00	0.01	0.00
Cr	0.00	0.00	0.00	0.00	0.00	0.00	0.00	0.00	0.00	0.00	0.00	0.00	0.00	0.00	0.00	0.00
Fe^{3+}	0.00	0.00	0.00	0.00	0.00	0.00	0.00	0.00	0.00	0.00	0.00	0.00	0.01	0.00	0.00	0.03
Fe^{2+}	2.13	2.15	1.99	2.10	2.37	2.21	2.26	2.21	2.24	2.29	2.14	2.09	2.06	2.29	1.70	1.27
Mn	0.11	0.22	0.75	0.06	0.20	0.08	0.03	0.15	0.13	0.12	0.05	0.07	0.05	0.14	0.36	1.15
Mg	0.49	0.40	0.20	0.54	0.32	0.44	0.48	0.41	0.42	0.45	0.53	0.55	0.54	0.43	0.15	0.43
Ni	0.00	0.00	0.00	0.00	0.00	0.00	0.00	0.00	0.00	0.00	0.00	0.00	0.00	0.00	0.00	0.00
Zn	0.00	0.00	0.00	0.00	0.00	0.00	0.00	0.00	0.00	0.00	0.00	0.00	0.00	0.00	0.00	0.00
Ca	0.25	0.21	0.06	0.27	0.08	0.27	0.20	0.20	0.20	0.12	0.26	0.27	0.36	0.14	0.78	0.17
Total	8.00	8.00	8.01	7.99	8.00	8.00	7.99	7.99	8.00	8.00	8.00	8.00	8.00	8.00	7.99	8.01
End members																
Almandine	71.49	72.23	66.12	70.60	79.85	73.88	75.90	74.49	74.91	76.79	71.78	69.98	68.43	76.53	56.89	41.42
Andradite	0.00	0.00	0.00	0.00	0.00	0.00	0.00	0.00	0.00	0.00	0.00	0.00	0.46	0.00	0.00	1.28
Grossular	8.18	7.21	2.13	9.23	2.60	8.79	6.85	6.62	6.61	3.91	8.63	9.16	11.51	4.63	26.12	4.40
Pyrope	16.43	13.34	6.62	18.17	10.77	14.61	16.19	13.73	13.95	15.20	17.85	18.37	17.93	14.27	4.99	14.32
Spessartine	3.83	7.23	25.13	2.00	6.71	2.63	1.05	5.14	4.46	4.03	1.71	2.47	1.52	4.57	11.99	38.58
Uvarovite	0.07	0.00	0.01	0.00	0.07	0.09	0.00	0.02	0.06	0.08	0.02	0.02	0.13	0.00	0.00	0.00
% cations	99.50	99.27	99.34	99.11	99.19	99.57	99.47	98.93	99.69	99.44	99.60	99.78	99.62	99.71	99.60	99.24
*calculated																

Supplementary Table S2

Representative microprobe analyses of detrital tourmalines from Upper Cretaceous to Paleocene deposits of the Jarmuta-Proč Fm., structural drill JAR-2, Pieniny sector of the PKB, Western Carpathians, Slovakia

Locality	Jarabina JAR-2	Jarabina JAR-2	Jarabina JAR-2	Jarabina JAR-2	Jarabina JAR-2	Jarabina JAR-2	Jarabina JAR-2	Jarabina JAR-2	Jarabina JAR-2	Jarabina JAR-2	Jarabina JAR-2	Jarabina JAR-2	Jarabina JAR-2	Jarabina JAR-2
Formation	Jarmuta-Proč Fm.	Jarmuta-Proč Fm.	Jarmuta-Proč Fm.	Jarmuta-Proč Fm.	Jarmuta-Proč Fm.	Jarmuta-Proč Fm.	Jarmuta-Proč Fm.	Jarmuta-Proč Fm.	Jarmuta-Proč Fm.	Jarmuta-Proč Fm.	Jarmuta-Proč Fm.	Jarmuta-Proč Fm.	Jarmuta-Proč Fm.	Jarmuta-Proč Fm.
Age	Maastrichtian–Middle Eocene	Maastrichtian–Middle Eocene	Maastrichtian–Middle Eocene	Maastrichtian–Middle Eocene	Maastrichtian–Middle Eocene	Maastrichtian–Middle Eocene	Maastrichtian–Middle Eocene	Maastrichtian–Middle Eocene	Maastrichtian–Middle Eocene	Maastrichtian–Middle Eocene	Maastrichtian–Middle Eocene	Maastrichtian–Middle Eocene	Maastrichtian–Middle Eocene	Maastrichtian–Middle Eocene
Unit	Šariš U.	Šariš U.	Šariš U.	Šariš U.	Šariš U.	Šariš U.	Šariš U.	Šariš U.	Šariš U.	Šariš U.	Šariš U.	Šariš U.	Šariš U.	Šariš U.
Sample	JAR-2A	JAR-2A	JAR-2A	JAR-2A	JAR-2A	JAR-2A	JAR-2A	JAR-2A	JAR-2A	JAR-2A	JAR-2A	JAR-2A	JAR-2A	JAR-2A
Point	an1	an2	an3	an4	an7	an9	an10	an12	an13	an30	an31	an32	an33	an34
Mineral	Srl	Foi	Mg-Foi	Vac-Mg-O root	Foi	Vac-Mg-O root	Vac-Mg-O root	Mg-Foi	Vac-Mg-O root	Mg-Foi	Drv	Vac-Mg-O root	Vac-Mg-O root	Drv
SiO_2	36.27	35.14	36.27	36.34	35.48	37.53	37.62	37.14	37.02	36.53	36.56	37.05	38.22	36.62
TiO_2	0.67	0.68	0.96	0.61	0.22	0.10	0.19	0.45	0.58	0.38	0.91	0.56	0.49	0.08
Al_2O_3	31.48	28.35	30.88	33.70	30.93	33.24	34.02	33.00	33.51	29.49	31.37	31.72	29.04	30.01
V_2O_3	0.03	0.03	0.02	0.05	0.04	0.02	0.00	0.02	0.05	0.07	0.01	0.05	0.06	0.03
Cr_2O_3	0.03	0.00	0.05	0.01	0.00	0.02	0.00	0.01	0.02	0.03	0.04	0.02	0.00	0.00
FeO	10.23	12.95	8.84	5.48	13.44	2.77	2.92	3.36	5.21	9.14	8.00	7.85	7.28	8.73
MnO	0.03	0.04	0.02	0.00	0.10	0.00	0.00	0.00	0.05	0.16	0.04	0.02	0.00	0.05
ZnO	0.04	0.05	0.00	0.00	0.21	0.08	0.00	0.07	0.13	0.00	0.02	0.00	0.05	0.01
CuO	0.00	0.00	0.00	0.01	0.00	0.00	0.00	0.02	0.03	0.00	0.03	0.00	0.03	0.07
MgO	5.01	4.86	6.15	6.57	3.15	9.32	8.38	8.75	7.04	7.60	6.37	6.75	7.92	7.29
CaO	0.12	1.29	0.51	0.58	0.53	0.02	0.05	0.63	0.55	0.57	0.11	0.09	0.09	0.03
BaO	0.00	0.03	0.00	0.00	0.00	0.05	0.00	0.00	0.07	0.00	0.01	0.00	0.08	0.00
Na_2O	2.45	1.08	1.34	0.99	1.27	1.31	1.56	1.25	1.17	1.29	2.39	1.42	1.47	2.99
K_2O	0.01	0.06	0.01	0.01	0.06	0.01	0.01	0.05	0.02	0.03	0.01	0.02	0.01	0.01
F	0.13	0.09	0.00	0.09	0.29	0.01	0.00	0.05	0.04	0.06	0.20	0.17	0.24	0.00
Cl	0.01	0.01	0.00	0.01	0.01	0.01	0.00	0.01	0.01	0.00	0.01	0.01	0.04	0.02
H_2O^*	3.37	3.10	3.17	3.07	2.97	3.17	3.24	3.22	3.18	3.17	3.33	3.09	3.05	3.58
$B_2O_3^*$	10.43	10.108	10.428	10.537	10.233	10.786	10.752	10.695	10.661	10.515	10.487	10.607	10.522	10.468
O = F	0.06	0.04	0.00	0.04	0.12	0.01	0.00	0.02	0.02	0.02	0.08	0.07	0.10	0.00
Total [%]	100.26	97.83	98.63	97.99	98.82	98.44	98.75	98.69	99.31	99.01	99.79	99.34	98.46	99.98
Si	6.04	6.04	6.04	5.99	6.03	6.05	6.08	6.04	6.04	6.04	6.06	6.07	6.31	6.08
Al	0.00	0.00	0.00	0.01	0.00	0.00	0.00	0.00	0.00	0.00	0.00	0.00	0.00	0.00
T-sum	6.044	6.042	6.044	6	6.026	6.048	6.082	6.035	6.035	6.037	6.059	6.07	6.313	6.08
B	3.00	3.00	3.00	3.00	3.00	3.00	3.00	3.00	3.00	3.00	3.00	3.00	3.00	3.00
Al	6.00	5.74	6.00	6.00	6.00	6.00	6.00	6.00	6.00	5.74	6.00	6.00	5.65	5.87
Cr	0.00	0.00	0.00	0.00	0.00	0.00	0.00	0.00	0.00	0.00	0.00	0.00	0.00	0.00
Mg	0	0.252	0	0	0	0	0	0	0	0.243	0	0	0.338	0.123
Fe^{3+}	0.00	0.00	0.00	0.00	0.00	0.00	0.00	0.00	0.00	0.00	0.00	0.00	0.00	0.00
Z-sum	6.00	6.00	6.00	6.00	6.00	6.00	6.00	6.00	6.00	6.00	6.00	6.00	6.00	6.00
Al	0.18	0.00	0.07	0.55	0.19	0.31	0.48	0.32	0.44	0.00	0.13	0.12	0.00	0.00
Ti	0.08	0.09	0.12	0.08	0.03	0.01	0.02	0.05	0.07	0.05	0.11	0.07	0.06	0.01
Fe^{3+}	0.00	0.00	0.00	0.00	0.00	0.00	0.00	0.00	0.00	0.00	0.00	0.00	0.00	0.00
Fe^{2+}	1.43	1.86	1.23	0.76	1.91	0.37	0.40	0.46	0.71	1.26	1.11	1.08	1.01	1.21
Mn^{2+}	0.01	0.01	0.00	0.00	0.02	0.00	0.00	0.00	0.01	0.02	0.01	0.00	0.00	0.01
Mg	1.246	0.995	1.527	1.614	0.799	2.24	2.019	2.119	1.71	1.63	1.574	1.649	1.612	1.68
Y-sum	2.96	2.96	2.96	3.00	2.97	2.95	2.92	2.97	2.97	2.96	2.94	2.93	2.69	2.92
Ca	0.02	0.24	0.09	0.10	0.10	0.00	0.01	0.11	0.10	0.10	0.02	0.02	0.02	0.01
Na	0.79	0.36	0.43	0.32	0.42	0.41	0.49	0.39	0.37	0.42	0.77	0.45	0.47	0.96
K	0.00	0.01	0.00	0.00	0.01	0.00	0.00	0.01	0.01	0.01	0.00	0.00	0.00	0.00
X-vacancy	0.19	0.39	0.47	0.58	0.47	0.58	0.50	0.49	0.53	0.48	0.21	0.53	0.51	0.03
X-sum	1.00	1.00	1.00	1.00	1.00	1.00	1.00	1.00	1.00	1.00	1.00	1.00	1.00	1.00
OH	3.74	3.56	3.53	3.37	3.37	3.41	3.50	3.49	3.45	3.49	3.69	3.38	3.36	3.96
O	0.19	0.39	0.47	0.58	0.47	0.58	0.50	0.49	0.53	0.48	0.21	0.53	0.51	0.03
V + W	4.00	4.00	4.00	4.00	4.00	4.00	4.00	4.00	4.00	4.00	4.00	4.00	4.00	4.00
*calculated														

Supplementary Table S2 – continuation

Locality	Jarabina JAR-2	Jarabina JAR-2	Jarabina JAR-2	Jarabina JAR-2	Jarabina JAR-2	Jarabina JAR-2	Jarabina JAR-2	Jarabina JAR-2	Jarabina JAR-2	Jarabina JAR-2	Jarabina JAR-2	Jarabina JAR-2	Jarabina JAR-2	Jarabina JAR-2
Formation	Jarmuta-Proč Fm.	Jarmuta-Proč Fm.	Jarmuta-Proč Fm.	Jarmuta-Proč Fm.	Jarmuta-Proč Fm.	Jarmuta-Proč Fm.	Jarmuta-Proč Fm.	Jarmuta-Proč Fm.	Jarmuta-Proč Fm.	Jarmuta-Proč Fm.	Jarmuta-Proč Fm.	Jarmuta-Proč Fm.	Jarmuta-Proč Fm.	Jarmuta-Proč Fm.
Age	Maastrichtian–Middle Eocene	Maastrichtian–Middle Eocene	Maastrichtian–Middle Eocene	Maastrichtian–Middle Eocene	Maastrichtian–Middle Eocene	Maastrichtian–Middle Eocene	Maastrichtian–Middle Eocene	Maastrichtian–Middle Eocene	Maastrichtian–Middle Eocene	Maastrichtian–Middle Eocene	Maastrichtian–Middle Eocene	Maastrichtian–Middle Eocene	Maastrichtian–Middle Eocene	Maastrichtian–Middle Eocene
Unit	Šariš U.	Šariš U.	Šariš U.	Šariš U.	Šariš U.	Šariš U.	Šariš U.	Šariš U.	Šariš U.	Šariš U.	Šariš U.	Šariš U.	Šariš U.	Šariš U.
Sample	JAR-2A	JAR-2A	JAR-2A	JAR-2B	JAR-2B	JAR-2B	JAR-2B	JAR-2B	JAR-2B	JAR-2B	JAR-2B	JAR-2B	JAR-2B	JAR-2B
Point	an36	an37	an38	an4	an5	an8	an9	an10	an11	an18	an20	an22	an23	an24
Mineral	Vac-Mg-O root	Vac-Mg-O root	Srl	Vac-Mg-O root	Srl	Vac-Mg-O root	Srl	Mg-Foi	Vac-Mg-O root	Vac-Mg-O root	Vac-Mg-O root	Vac-Mg-O root	Vac-Mg-O root	Vac-Mg-O root
SiO_2	36.97	34.31	36.51	36.35	35.47	36.48	36.35	36.03	36.13	36.89	36.84	36.54	36.64	36.67
TiO_2	0.58	1.22	0.41	0.59	0.15	0.28	0.82	0.80	0.28	0.67	0.91	0.36	0.31	0.32
Al_2O_3	34.31	26.50	28.16	31.41	27.77	32.06	28.23	30.43	32.44	32.06	30.91	34.76	34.43	31.51
V_2O_3	0.16	0.04	0.04	0.06	0.07	0.00	0.05	0.00	0.04	0.01	0.04	0.00	0.13	0.01
Cr_2O_3	0.32	0.01	0.02	0.04	0.00	0.04	0.02	0.00	0.03	0.01	0.04	0.00	0.04	0.02
FeO	3.10	11.96	11.92	9.30	12.27	9.45	10.34	8.92	7.11	5.25	7.77	7.94	7.34	9.21
MnO	0.01	0.00	0.05	0.00	0.03	0.02	0.00	0.07	0.05	0.05	0.01	0.00	0.07	0.05
ZnO	0.08	0.06	0.04	0.00	0.00	0.03	0.07	0.04	0.01	0.08	0.07	0.05	0.04	0.00
CuO	0.00	0.04	0.00	0.00	0.00	0.01	0.00	0.00	0.04	0.01	0.02	0.00	0.00	0.06
MgO	8.11	5.49	5.53	5.51	6.42	5.58	6.70	6.24	6.92	7.95	6.74	4.51	4.92	5.99
CaO	0.40	0.09	0.07	0.34	0.97	0.13	0.18	0.43	0.49	0.65	0.28	0.29	0.31	0.13
BaO	0.00	0.01	0.01	0.00	0.00	0.10	0.00	0.00	0.04	0.00	0.00	0.10	0.12	0.00
Na_2O	1.06	1.37	2.63	1.24	1.24	1.33	1.49	1.35	1.21	1.19	1.39	0.80	1.03	1.44
K_2O	0.04	0.03	0.39	0.01	0.01	0.02	0.02	0.02	0.06	0.01	0.01	0.01	0.01	0.02
F	0.08	0.00	0.00	0.05	0.00	0.02	0.00	0.00	0.26	0.13	0.15	0.00	0.00	0.12
Cl	0.01	0.02	0.02	0.00	0.01	0.00	0.00	0.00	0.00	0.00	0.01	0.01	0.00	0.00
H_2O^*	3.13	2.96	3.50	3.09	3.16	3.13	3.13	3.14	3.05	3.14	3.10	3.02	3.09	3.11
$B_2O_3^*$	10.774	9.821	10.237	10.414	10.223	10.518	10.31	10.352	10.541	10.609	10.5	10.565	10.56	10.517
O = F	0.04	0.00	0.00	0.02	0.00	0.01	0.00	0.00	0.11	0.06	0.06	0.00	0.00	0.05
Total [%]	99.11	93.92	99.53	98.39	97.80	99.18	97.70	97.82	98.59	98.68	98.69	98.95	99.04	99.10
Si	5.96	6.07	6.20	6.07	6.03	6.03	6.13	6.05	5.96	6.04	6.10	6.01	6.03	6.06
Al	0.04	0.00	0.00	0.00	0.00	0.00	0.00	0.00	0.04	0.00	0.00	0.00	0.00	0.00
T-sum	6	6.072	6.199	6.067	6.031	6.028	6.127	6.048	6	6.044	6.097	6.011	6.029	6.059
B	3.00	3.00	3.00	3.00	3.00	3.00	3.00	3.00	3.00	3.00	3.00	3.00	3.00	3.00
Al	6.00	5.53	5.64	6.00	5.57	6.00	5.61	6.00	6.00	6.00	6.00	6.00	6.00	6.00
Cr	0.00	0.00	0.00	0.00	0.00	0.00	0.00	0.00	0.00	0.00	0.00	0.00	0.00	0.00
Mg	0	0.465	0.357	0	0.425	0	0.381	0	0	0	0	0	0	0
Fe^{3+}	0.00	0.00	0.00	0.00	0.00	0.00	0.00	0.00	0.00	0.00	0.00	0.00	0.00	0.00
Z-sum	6.00	6.00	6.00	6.00	6.00	6.00	6.00	6.00	6.00	6.00	6.00	6.00	6.00	6.00
Al	0.49	0.00	0.00	0.18	0.00	0.24	0.00	0.02	0.27	0.19	0.03	0.74	0.68	0.14
Ti	0.07	0.16	0.05	0.08	0.02	0.03	0.10	0.10	0.03	0.08	0.11	0.04	0.04	0.04
Fe^{3+}	0.00	0.00	0.00	0.00	0.00	0.00	0.00	0.00	0.00	0.00	0.00	0.00	0.00	0.00
Fe^{2+}	0.42	1.77	1.69	1.30	1.74	1.31	1.46	1.25	0.98	0.72	1.08	1.09	1.01	1.27
Mn^{2+}	0.00	0.00	0.01	0.00	0.00	0.00	0.00	0.01	0.01	0.01	0.00	0.00	0.01	0.01
Mg	1.951	0.983	1.043	1.372	1.201	1.375	1.302	1.561	1.7	1.943	1.662	1.106	1.208	1.475
Y-sum	3.00	2.93	2.80	2.93	2.97	2.97	2.87	2.95	3.01	2.96	2.90	2.99	2.97	2.94
Ca	0.07	0.02	0.01	0.06	0.18	0.02	0.03	0.08	0.09	0.12	0.05	0.05	0.05	0.02
Na	0.33	0.47	0.86	0.40	0.41	0.43	0.49	0.44	0.39	0.38	0.45	0.25	0.33	0.46
K	0.01	0.01	0.09	0.00	0.00	0.00	0.00	0.00	0.01	0.00	0.00	0.00	0.00	0.00
X-vacancy	0.59	0.51	0.04	0.53	0.41	0.54	0.48	0.48	0.51	0.51	0.50	0.69	0.61	0.51
X-sum	1.00	1.00	1.00	1.00	1.00	1.00	1.00	1.00	1.00	1.00	1.00	1.00	1.00	1.00
OH	3.37	3.49	3.96	3.44	3.59	3.45	3.52	3.52	3.36	3.43	3.42	3.31	3.39	3.43
O	0.59	0.51	0.04	0.53	0.41	0.54	0.48	0.48	0.51	0.51	0.50	0.69	0.61	0.51
V + W	4.00	4.00	4.00	4.00	4.00	4.00	4.00	4.00	4.00	4.00	4.00	4.00	4.00	4.00
*calculated														

Supplementary Table S2 – continuation

Locality	Jarabina JAR-2	Jarabina JAR-2	Jarabina JAR-2	Jarabina JAR-2	Jarabina JAR-2	Jarabina JAR-2	Jarabina JAR-2	Jarabina JAR-2	Jarabina JAR-2	Jarabina JAR-2	Jarabina JAR-2	Jarabina JAR-2	Jarabina JAR-2	Jarabina JAR-2
Formation	Jarmuta-Proč Fm.	Jarmuta-Proč Fm.	Jarmuta-Proč Fm.	Jarmuta-Proč Fm.	Jarmuta-Proč Fm.	Jarmuta-Proč Fm.	Jarmuta-Proč Fm.	Jarmuta-Proč Fm.	Jarmuta-Proč Fm.	Jarmuta-Proč Fm.	Jarmuta-Proč Fm.	Jarmuta-Proč Fm.	Jarmuta-Proč Fm.	Jarmuta-Proč Fm.
Age	Maastrichtian–Middle Eocene	Maastrichtian–Middle Eocene	Maastrichtian–Middle Eocene	Maastrichtian–Middle Eocene	Maastrichtian–Middle Eocene	Maastrichtian–Middle Eocene	Maastrichtian–Middle Eocene	Maastrichtian–Middle Eocene	Maastrichtian–Middle Eocene	Maastrichtian–Middle Eocene	Maastrichtian–Middle Eocene	Maastrichtian–Middle Eocene	Maastrichtian–Middle Eocene	Maastrichtian–Middle Eocene
Unit	Šariš U.	Šariš U.	Šariš U.	Šariš U.	Šariš U.	Šariš U.	Šariš U.	Šariš U.	Šariš U.	Šariš U.	Šariš U.	Šariš U.	Šariš U.	Šariš U.
Sample	JAR-2B	JAR-2B	JAR-2B	JAR-2B	JAR-2B	JAR-2B	JAR-2B	JAR-2C	JAR-2C	JAR-2C	JAR-2C	JAR-2C	JAR-2C	JAR-2C
Point	an25	an27	an28	an30	an31	an32	an33	an7	an11	an12	an13	an14	an15	an25
Mineral	Vac-Mg-O root	Vac-Mg-O root	Mg-Foi	Vac-Mg-O root	Vac-Mg-O root	Vac-Mg-O root	Mg-Foi	Drv	Vac-Fe-O root	Vac-Mg-O root	Vac-Fe-O root	Drv	Srl	Foi
SiO_2	36.34	34.78	36.98	36.29	36.20	36.73	36.45	36.62	36.76	36.74	34.43	36.85	35.85	35.36
TiO_2	0.88	0.60	0.97	0.90	0.87	0.30	0.75	1.19	0.34	0.86	0.15	0.00	0.54	0.52
Al_2O_3	32.57	34.02	31.20	34.16	34.85	35.29	32.37	30.97	32.74	32.77	34.48	31.73	27.57	33.33
V_2O_3	0.05	0.00	0.03	0.01	0.07	0.03	0.02	0.10	0.00	0.04	0.00	0.03	0.08	0.03
Cr_2O_3	0.01	0.02	0.04	0.04	0.11	0.06	0.04	0.04	0.00	0.03	0.01	0.00	0.00	0.00
FeO	8.79	11.24	7.67	6.05	7.55	6.90	4.91	8.49	9.27	5.63	14.49	8.14	12.37	9.70
MnO	0.05	0.05	0.02	0.09	0.00	0.00	0.10	0.03	0.07	0.00	0.19	0.04	0.05	0.02
ZnO	0.05	0.10	0.02	0.06	0.00	0.07	0.03	0.00	0.05	0.03	0.15	0.04	0.00	0.16
CuO	0.00	0.00	0.00	0.00	0.02	0.00	0.00	0.00	0.00	0.00	0.01	0.00	0.00	0.00
MgO	5.53	3.02	6.97	6.50	4.68	4.73	7.65	6.78	5.11	6.92	0.30	6.85	6.16	4.40
CaO	0.66	0.55	0.60	0.70	0.47	0.21	0.44	0.33	0.14	0.31	0.24	0.23	0.35	0.96
BaO	0.03	0.00	0.00	0.00	0.00	0.00	0.00	0.03	0.01	0.01	0.00	0.00	0.00	0.03
Na_2O	0.94	1.01	1.30	1.00	0.95	0.91	1.36	2.52	1.22	1.14	1.01	2.86	2.76	1.00
K_2O	0.01	0.05	0.01	0.02	0.01	0.01	0.02	0.01	0.01	0.01	0.04	0.03	0.03	0.05
F	0.12	0.24	0.00	0.07	0.00	0.00	0.02	0.13	0.05	0.10	0.00	0.00	0.02	0.00
Cl	0.00	0.01	0.00	0.01	0.01	0.01	0.01	0.00	0.01	0.00	0.00	0.01	0.01	0.00
H_2O^*	3.06	2.96	3.21	3.14	3.09	3.04	3.18	3.47	3.08	3.07	2.98	3.61	3.51	3.15
$B_2O_3^*$	10.557	10.356	10.587	10.675	10.587	10.602	10.522	10.585	10.552	10.555	10.201	10.585	10.241	10.413
O = F	0.05	0.10	0.00	0.03	0.00	0.00	0.01	0.06	0.02	0.04	0.00	0.00	0.01	0.00
Total [%]	99.60	98.91	99.61	99.68	99.46	98.89	97.83	101.23	99.40	98.16	98.68	100.99	99.54	99.13
Si	5.98	5.84	6.07	5.91	5.94	6.02	6.02	6.01	6.06	6.05	5.87	6.05	6.09	5.90
Al	0.02	0.16	0.00	0.09	0.06	0.00	0.00	0.00	0.00	0.00	0.13	0.00	0.00	0.10
T-sum	6	6	6.071	6	6	6.022	6.02	6.013	6.055	6.049	6	6.05	6.085	6
B	3.00	3.00	3.00	3.00	3.00	3.00	3.00	3.00	3.00	3.00	3.00	3.00	3.00	3.00
Al	6.00	6.00	6.00	6.00	6.00	6.00	6.00	5.99	6.00	6.00	6.00	6.00	5.51	6.00
Cr	0.00	0.00	0.00	0.00	0.00	0.00	0.00	0.01	0.00	0.00	0.00	0.00	0.00	0.00
Mg	0	0	0	0	0	0	0	0	0	0	0	0	0.475	0
Fe^{3+}	0.00	0.00	0.00	0.00	0.00	0.00	0.00	0.00	0.00	0.00	0.00	0.00	0.00	0.00
Z-sum	6.00	6.00	6.00	6.00	6.00	6.00	6.00	6.00	6.00	6.00	6.00	6.00	6.00	6.00
Al	0.30	0.57	0.04	0.46	0.69	0.82	0.30	0.00	0.36	0.36	0.79	0.14	0.00	0.46
Ti	0.11	0.08	0.12	0.11	0.11	0.04	0.09	0.15	0.04	0.11	0.02	0.00	0.07	0.07
Fe^{3+}	0.00	0.00	0.00	0.00	0.00	0.00	0.00	0.00	0.00	0.00	0.00	0.00	0.00	0.00
Fe^{2+}	1.21	1.58	1.05	0.82	1.04	0.95	0.68	1.17	1.28	0.78	2.06	1.12	1.76	1.35
Mn^{2+}	0.01	0.01	0.00	0.01	0.00	0.00	0.01	0.00	0.01	0.00	0.03	0.01	0.01	0.00
Mg	1.358	0.755	1.706	1.577	1.145	1.157	1.883	1.659	1.255	1.699	0.077	1.677	1.083	1.094
Y-sum	3.00	3.00	2.93	3.00	3.00	2.98	2.98	2.99	2.95	2.95	3.00	2.95	2.92	3.00
Ca	0.12	0.10	0.11	0.12	0.08	0.04	0.08	0.06	0.03	0.06	0.04	0.04	0.06	0.17
Na	0.30	0.33	0.41	0.32	0.30	0.29	0.43	0.80	0.39	0.37	0.33	0.91	0.91	0.32
K	0.00	0.01	0.00	0.01	0.00	0.00	0.00	0.00	0.00	0.00	0.01	0.01	0.01	0.01
X-vacancy	0.58	0.56	0.48	0.56	0.61	0.67	0.49	0.14	0.58	0.58	0.62	0.05	0.02	0.49
X-sum	1.00	1.00	1.00	1.00	1.00	1.00	1.00	1.00	1.00	1.00	1.00	1.00	1.00	1.00
OH	3.36	3.31	3.52	3.41	3.39	3.33	3.51	3.80	3.39	3.37	3.38	3.95	3.97	3.51
O	0.58	0.56	0.48	0.56	0.61	0.67	0.49	0.14	0.58	0.58	0.62	0.05	0.02	0.49
V + W	4.00	4.00	4.00	4.00	4.00	4.00	4.00	4.00	4.00	4.00	4.00	4.00	4.00	4.00
*calculated														

Supplementary Table S2 – continuation

Locality	Ľutina	Ľutina	Ľutina	Ľutina	Ľutina	Ľutina	Ľutina	Ľutina	Ľutina	Ľutina	Ľutina	Ľutina	Ľutina	Ľutina
Formation	Malinowa Fm.	Malinowa Fm.	Malinowa Fm.	Malinowa Fm.	Malinowa Fm.	Malinowa Fm.	Malinowa Fm.	Malinowa Fm.	Malinowa Fm.	Malinowa Fm.	Malinowa Fm.	Malinowa Fm.	Malinowa Fm.	Malinowa Fm.
Age	Turonian–Campanian	Turonian–Campanian	Turonian–Campanian	Turonian–Campanian	Turonian–Campanian	Turonian–Campanian	Turonian–Campanian	Turonian–Campanian	Turonian–Campanian	Turonian–Campanian	Turonian–Campanian	Turonian–Campanian	Turonian–Campanian	Turonian–Campanian
Unit	Šariš U.	Šariš U.	Šariš U.	Šariš U.	Šariš U.	Šariš U.	Šariš U.	Šariš U.	Šariš U.	Šariš U.	Šariš U.	Šariš U.	Šariš U.	Šariš U.
Sample	JAR-2C	JAR-2C	JAR-2C	JAR-2C	JAR-2C	JAR-2C	JAR-2C	JAR-2C	LU-5A	LU-5A	LU-5A	LU-5A	LU-5A	LU-5A
Point	an26	an27	an28	an30	an31	an32	an33	an34	an1	an2	an3	an4	an5	an6
Mineral	Vac-Mg-O root	Drv	Drv	Mg-Foi	Srl	Vac-Mg-O root	Mg-Foi	Vac-Fe-O root	Vac-Mg-O root	Feruvi	Foi	Foi	Srl	Vac-Mg-O root
SiO_2	36.80	36.47	36.80	36.65	35.48	36.11	36.88	36.18	36.28	35.07	34.23	35.79	35.90	36.06
TiO_2	0.23	0.57	0.22	0.77	1.22	0.98	0.90	0.71	1.06	0.92	0.39	0.15	0.34	0.56
Al_2O_3	33.04	30.70	30.10	30.53	27.24	33.74	31.00	34.22	29.74	24.90	24.03	27.91	29.35	29.87
V_2O_3	0.03	0.06	0.01	0.07	0.04	0.06	0.06	0.03	0.02	0.02	0.03	0.00	0.08	0.04
Cr_2O_3	0.05	0.06	0.04	0.01	0.00	0.07	0.02	0.03	0.09	0.00	0.01	0.00	0.01	0.00
FeO	6.91	8.15	6.22	7.72	14.34	7.65	4.95	8.09	9.08	15.71	21.45	12.69	12.84	10.11
MnO	0.00	0.04	0.11	0.09	0.07	0.00	0.00	0.17	0.01	0.02	0.00	0.05	0.00	0.02
ZnO	0.00	0.08	0.00	0.04	0.00	0.03	0.04	0.00	0.00	0.05	0.08	0.04	0.04	0.03
CuO	0.00	0.00	0.00	0.04	0.00	0.00	0.00	0.08	0.28	0.02	0.04	0.04	0.00	0.01
MgO	6.45	6.84	9.31	6.87	4.36	5.21	8.51	4.42	6.45	5.02	2.67	6.07	4.67	5.95
CaO	0.42	0.22	0.28	0.49	0.45	0.73	0.49	0.19	0.33	2.13	1.03	1.00	0.22	0.19
BaO	0.00	0.01	0.00	0.02	0.00	0.00	0.00	0.00	0.00	0.00	0.00	0.05	0.02	0.00
Na_2O	1.10	2.66	2.74	1.35	1.43	1.01	1.35	1.20	1.30	0.88	1.07	1.18	1.46	1.29
K_2O	0.03	0.01	0.02	0.00	0.04	0.03	0.04	0.04	0.02	0.04	0.08	0.03	0.03	0.01
F	0.11	0.10	0.00	0.06	0.00	0.14	0.07	0.04	0.17	0.00	0.00	0.04	0.07	0.04
Cl	0.00	0.01	0.01	0.01	0.00	0.00	0.00	0.00	0.00	0.02	0.00	0.00	0.00	0.00
H_2O^*	3.08	3.47	3.59	3.15	3.10	3.08	3.17	3.09	3.04	3.18	3.04	3.15	3.09	3.06
$B_2O_3^*$	10.588	10.46	10.621	10.44	10.088	10.532	10.546	10.505	10.385	9.944	9.836	10.261	10.26	10.322
O = F	0.05	0.04	0.00	0.03	0.00	0.06	0.03	0.02	0.07	0.00	0.00	0.02	0.03	0.02
Total [%]	98.80	99.85	100.08	98.28	97.84	99.29	98.01	98.99	98.18	97.93	97.98	98.44	98.34	97.53
Si	6.04	6.06	6.02	6.10	6.11	5.96	6.08	5.99	6.07	6.13	6.05	6.06	6.08	6.07
Al	0.00	0.00	0.00	0.00	0.00	0.04	0.00	0.01	0.00	0.00	0.00	0.00	0.00	0.00
T-sum	6.04	6.059	6.023	6.101	6.112	6	6.078	6	6.071	6.13	6.048	6.062	6.081	6.072
B	3.00	3.00	3.00	3.00	3.00	3.00	3.00	3.00	3.00	3.00	3.00	3.00	3.00	3.00
Al	6.00	6.00	5.81	5.99	5.53	6.00	6.00	6.00	5.87	5.13	5.01	5.57	5.86	5.93
Cr	0.00	0.00	0.01	0.00	0.00	0.00	0.00	0.00	0.01	0.00	0.00	0.00	0.00	0.00
Mg	0	0	0.187	0	0.464	0	0	0	0.119	0.867	0.704	0.428	0.128	0.068
Fe^{3+}	0.00	0.00	0.00	0.00	0.00	0.00	0.00	0.00	0.00	0.00	0.00	0.00	0.00	0.00
Z-sum	6.00	6.00	6.00	6.00	6.00	6.00	6.00	6.00	6.00	6.00	6.00	6.00	6.00	6.00
Al	0.39	0.01	0.00	0.00	0.00	0.52	0.02	0.66	0.00	0.00	0.00	0.00	0.00	0.00
Ti	0.03	0.07	0.03	0.10	0.16	0.12	0.11	0.09	0.13	0.12	0.05	0.02	0.04	0.07
Fe^{3+}	0.00	0.00	0.00	0.00	0.00	0.00	0.00	0.00	0.00	0.00	0.00	0.00	0.00	0.00
Fe^{2+}	0.95	1.13	0.85	1.08	2.07	1.06	0.68	1.12	1.27	2.30	2.89	1.80	1.82	1.42
Mn^{2+}	0.00	0.01	0.02	0.01	0.01	0.00	0.00	0.02	0.00	0.00	0.00	0.01	0.00	0.00
Mg	1.579	1.695	2.083	1.705	0.655	1.282	2.091	1.091	1.489	0.44	0	1.105	1.053	1.425
Y-sum	2.96	2.94	2.98	2.90	2.89	3.00	2.92	3.00	2.93	2.87	2.95	2.94	2.92	2.93
Ca	0.07	0.04	0.05	0.09	0.08	0.13	0.09	0.03	0.06	0.40	0.20	0.18	0.04	0.03
Na	0.35	0.86	0.87	0.44	0.48	0.32	0.43	0.39	0.42	0.30	0.37	0.39	0.48	0.42
K	0.01	0.00	0.00	0.00	0.01	0.01	0.01	0.01	0.01	0.01	0.02	0.01	0.01	0.00
X-vacancy	0.57	0.10	0.08	0.47	0.43	0.54	0.47	0.57	0.51	0.29	0.42	0.42	0.47	0.54
X-sum	1.00	1.00	1.00	1.00	1.00	1.00	1.00	1.00	1.00	1.00	1.00	1.00	1.00	1.00
OH	3.37	3.84	3.92	3.49	3.57	3.39	3.49	3.41	3.40	3.70	3.58	3.56	3.49	3.44
O	0.57	0.10	0.08	0.47	0.43	0.54	0.47	0.57	0.51	0.29	0.42	0.42	0.47	0.54
V + W	4.00	4.00	4.00	4.00	4.00	4.00	4.00	4.00	4.00	4.00	4.00	4.00	4.00	4.00
*calculated														

Supplementary Table S2 – continuation

Locality	Ľutina	Ľutina	Ľutina	Ľutina	Ľutina	Ľutina	Ľutina	Ľutina	Ľutina	Ľutina	Ľutina	Ľutina
Formation	Malinowa Fm.	Malinowa Fm.	Malinowa Fm.	Malinowa Fm.	Malinowa Fm.	Malinowa Fm.	Malinowa Fm.	Malinowa Fm.	Malinowa Fm.	Malinowa Fm.	Malinowa Fm.	Malinowa Fm.
Age	Turonian–Campanian	Turonian–Campanian	Turonian–Campanian	Turonian–Campanian	Turonian–Campanian	Turonian–Campanian	Turonian–Campanian	Turonian–Campanian	Turonian–Campanian	Turonian–Campanian	Turonian–Campanian	Turonian–Campanian
Unit	Šariš U.	Šariš U.	Šariš U.	Šariš U.	Šariš U.	Šariš U.	Šariš U.	Šariš U.	Šariš U.	Šariš U.	Šariš U.	Šariš U.
Sample	LU-5A	LU-5A	LU-5A	LU-5A	LU-5A	LU-5A	LU-5A	LU-5A	LU-5A	LU-5A	LU-5B	LU-5B
Point	an7	an19	an20	an25	an26	an35	an36	an37	an38	an42	an6	an7
Mineral	Vac-Mg-O root	Mg-Foi	Uvi	Vac-Mg-O root	Drv	Drv	Srl	Srl	Srl	Vac-Fe-O root	Vac-Mg-O root	Vac-Mg-O root
SiO_2	36.03	36.75	35.43	36.56	37.06	36.90	35.76	36.30	35.98	35.90	36.23	36.35
TiO_2	0.60	0.44	1.55	0.96	0.25	0.19	0.44	0.34	0.41	0.17	1.31	0.48
Al_2O_3	31.91	32.31	25.94	33.34	31.53	30.05	26.96	28.16	27.29	35.23	30.55	35.11
V_2O_3	0.04	0.01	0.14	0.08	0.02	0.04	0.00	0.04	0.05	0.03	0.04	0.07
Cr_2O_3	0.08	0.00	0.01	0.09	0.06	0.00	0.02	0.01	0.03	0.00	0.00	0.08
FeO	7.50	6.08	9.56	4.43	6.31	8.33	12.39	12.28	13.16	10.98	9.50	5.30
MnO	0.04	0.01	0.00	0.03	0.00	0.03	0.00	0.00	0.09	0.06	0.00	0.07
ZnO	0.04	0.07	0.00	0.07	0.05	0.11	0.02	0.05	0.05	0.08	0.00	0.06
CuO	0.00	0.00	0.03	0.00	0.00	0.00	0.00	0.01	0.00	0.04	0.02	0.07
MgO	6.20	7.59	9.16	7.93	8.09	8.09	6.68	6.12	6.14	1.96	5.87	6.17
CaO	0.66	0.76	2.21	0.88	0.06	0.02	0.02	0.62	0.72	0.03	0.13	0.69
BaO	0.00	0.00	0.10	0.05	0.00	0.00	0.00	0.02	0.07	0.00	0.00	0.04
Na_2O	1.11	1.17	0.87	1.03	2.85	2.71	1.57	2.55	2.48	0.74	1.39	1.01
K_2O	0.00	0.03	0.08	0.03	0.01	0.03	0.06	0.03	0.04	0.03	0.01	0.04
F	0.01	0.10	0.06	0.03	0.00	0.02	0.03	0.00	0.00	0.12	0.18	0.12
Cl	0.01	0.00	0.01	0.00	0.00	0.00	0.01	0.00	0.00	0.00	0.00	0.01
H_2O^*	3.11	3.17	3.28	3.20	3.59	3.53	3.10	3.52	3.51	2.86	3.04	3.11
$B_2O_3^*$	10.401	10.618	10.308	10.694	10.642	10.615	10.221	10.34	10.29	10.41	10.43	10.66
O = F	0.00	0.04	0.03	0.01	0.00	0.01	0.01	0.00	0.00	0.05	0.08	0.05
Total [%]	97.75	99.07	98.70	99.38	100.52	100.65	97.26	100.36	100.30	98.59	98.63	99.36
Si	6.02	6.02	5.97	5.94	6.05	6.04	6.08	6.10	6.08	6.00	6.04	5.93
Al	0.00	0.00	0.01	0.06	0.00	0.00	0.00	0.00	0.00	0.01	0.00	0.07
T-sum	6.021	6.016	6	6	6.052	6.041	6.08	6.104	6.079	6	6.04	6
B	3.00	3.00	3.00	3.00	3.00	3.00	3.00	3.00	3.00	3.00	3.00	3.00
Al	6.00	6.00	5.15	6.00	6.00	5.80	5.40	5.58	5.43	6.00	6.00	6.00
Cr	0.00	0.00	0.00	0.00	0.00	0.00	0.00	0.00	0.00	0.00	0.00	0.00
Mg	0	0	0.832	0	0	0.197	0.594	0.414	0.555	0	0	0
Fe^{3+}	0.00	0.00	0.00	0.00	0.00	0.00	0.00	0.00	0.00	0.00	0.00	0.00
Z-sum	6.00	6.00	6.00	6.00	6.00	6.00	6.00	6.00	6.00	6.00	6.00	6.00
Al	0.28	0.23	0.00	0.33	0.07	0.00	0.00	0.00	0.00	0.93	0.00	0.67
Ti	0.08	0.05	0.20	0.12	0.03	0.02	0.06	0.04	0.05	0.02	0.16	0.06
Fe^{3+}	0.00	0.00	0.00	0.00	0.00	0.00	0.00	0.00	0.00	0.00	0.00	0.00
Fe^{2+}	1.05	0.83	1.35	0.60	0.86	1.14	1.76	1.73	1.86	1.53	1.33	0.72
Mn^{2+}	0.01	0.00	0.00	0.00	0.00	0.00	0.00	0.00	0.01	0.01	0.00	0.01
Mg	1.545	1.853	1.471	1.92	1.971	1.777	1.1	1.119	0.991	0.489	1.458	1.501
Y-sum	2.98	2.98	3.02	3.00	2.95	2.96	2.92	2.90	2.92	3.00	2.96	3.00
Ca	0.12	0.13	0.40	0.15	0.01	0.00	0.00	0.11	0.13	0.01	0.02	0.12
Na	0.36	0.37	0.28	0.33	0.90	0.86	0.52	0.83	0.81	0.24	0.45	0.32
K	0.00	0.01	0.02	0.01	0.00	0.01	0.01	0.01	0.01	0.01	0.00	0.01
X-vacancy	0.52	0.49	0.29	0.51	0.09	0.13	0.47	0.05	0.05	0.75	0.53	0.55
X-sum	1.00	1.00	1.00	1.00	1.00	1.00	1.00	1.00	1.00	1.00	1.00	1.00
OH	3.47	3.46	3.69	3.47	3.91	3.86	3.52	3.95	3.95	3.19	3.38	3.39
O	0.52	0.49	0.27	0.51	0.09	0.13	0.47	0.05	0.05	0.75	0.53	0.55
V + W	4.00	4.00	4.00	4.00	4.00	4.00	4.00	4.00	4.00	4.00	4.00	4.00
*calculated												

Supplementary Table S2 – continuation

Locality	Ľutina	Ľutina	Ľutina	Ľutina	Ľutina	Ľutina
Formation	Malinowa Fm.	Malinowa Fm.	Malinowa Fm.	Malinowa Fm.	Malinowa Fm.	Malinowa Fm.
Age	Turonian–Campanian	Turonian–Campanian	Turonian–Campanian	Turonian–Campanian	Turonian–Campanian	Turonian–Campanian
Unit	Šariš U.	Šariš U.	Šariš U.	Šariš U.	Šariš U.	Šariš U.
Sample	LU-5B	LU-5B	LU-5B	LU-5B	LU-5B	LU-5B
Point	an14	an15	an16	an22	an23	an29
Mineral	Drv	Mg-Foi	Srl	Mg-Foi	Drv	Vac-Mg-O root
SiO_2	37.26	35.50	35.57	36.06	36.79	36.97
TiO_2	0.88	1.22	0.73	0.60	1.07	0.64
Al_2O_3	33.74	34.23	25.68	28.84	32.12	33.69
V_2O_3	0.16	0.25	0.01	0.14	0.03	0.08
Cr_2O_3	0.13	0.23	0.00	0.01	0.07	0.03
FeO	4.69	7.78	15.10	9.73	5.46	7.58
MnO	0.00	0.00	0.01	0.06	0.00	0.08
ZnO	0.04	0.09	0.00	0.00	0.03	0.00
CuO	0.01	0.05	0.00	0.00	0.00	0.01
MgO	7.65	4.73	5.26	7.27	7.90	5.22
CaO	0.29	0.77	0.06	1.38	0.83	0.08
BaO	0.00	0.03	0.14	0.00	0.02	0.00
Na_2O	2.66	1.18	1.55	1.07	2.23	1.08
K2O	0.09	0.06	0.05	0.07	0.03	0.01
F	0.02	0.08	0.00	0.00	0.06	0.12
Cl	0.00	0.01	0.00	0.00	0.00	0.01
H_2O^*	3.62	3.16	3.08	3.23	3.52	3.01
$B_2O_3^*$	10.81	10.52	10.07	10.39	10.65	10.59
O = F	0.01	0.03	0.00	0.00	0.02	0.05
Total [%]	102.04	99.82	97.29	98.85	100.77	99.13
Si	5.99	5.87	6.14	6.04	6.01	6.07
Al	0.01	0.14	0.00	0.00	0.00	0.00
T-sum	6	6	6.142	6.035	6.006	6.066
B	3.00	3.00	3.00	3.00	3.00	3.00
Al	6.00	6.00	5.23	5.69	6.00	6.00
Cr	0.00	0.00	0.00	0.00	0.00	0.00
Mg	0	0	0.773	0.293	0	0
Fe^{3+}	0.00	0.00	0.00	0.00	0.00	0.00
Z-sum	6.00	6.00	6.00	6.00	6.00	6.00
Al	0.39	0.53	0.00	0.00	0.18	0.51
Ti	0.11	0.15	0.10	0.08	0.13	0.08
Fe^{3+}	0.00	0.00	0.00	0.00	0.00	0.00
Fe^{2+}	0.63	1.08	2.18	1.36	0.75	1.04
Mn^{2+}	0.00	0.00	0.00	0.01	0.00	0.01
Mg	1.835	1.165	0.581	1.519	1.922	1.276
Y-sum	3.00	3.00	2.86	2.97	2.99	2.93
Ca	0.05	0.14	0.01	0.25	0.15	0.01
Na	0.83	0.38	0.52	0.35	0.71	0.34
K	0.02	0.01	0.01	0.01	0.01	0.00
X-vacancy	0.10	0.48	0.45	0.39	0.14	0.64
X-sum	1.00	1.00	1.00	1.00	1.00	1.00
OH	3.89	3.48	3.55	3.61	3.83	3.29
O	0.10	0.48	0.45	0.39	0.14	0.64
V + W	4.00	4.00	4.00	4.00	4.00	4.00
*calculated						

Supplementary Table S3

Representative microprobe analyses of detrital chromian spinels from Upper Cretaceous to Paleocene deposits of the Jarmuta-Proč Fm., structural drill JAR-2, Pieniny sector of the PKB, Western Carpathians, Slovakia

Locality	Jarabina JAR-2	Jarabina JAR-2	Ľutina	Ľutina	Ľutina	Ľutina	Ľutina	Ľutina	Ľutina	Ľutina	Ľutina	Ľutina	Ľutina	Ľutina
Formation	Jarmuta-Proč Fm.	Jarmuta-Proč Fm.	Malinowa Fm.	Malinowa Fm.	Malinowa Fm.	Malinowa Fm.	Malinowa Fm.	Malinowa Fm.	Malinowa Fm.	Malinowa Fm.	Malinowa Fm.	Malinowa Fm.	Malinowa Fm.	Malinowa Fm.
Age	Maastrichtian–Middle Eocene	Maastrichtian–Middle Eocene	Turonian–Campanian	Turonian–Campanian	Turonian–Campanian	Turonian–Campanian	Turonian–Campanian	Turonian–Campanian	Turonian–Campanian	Turonian–Campanian	Turonian–Campanian	Turonian–Campanian	Turonian–Campanian	Turonian–Campanian
Unit	Šariš U.	Šariš U.	Šariš U.	Šariš U.	Šariš U.	Šariš U.	Šariš U.	Šariš U.	Šariš U.	Šariš U.	Šariš U.	Šariš U.	Šariš U.	Šariš U.
Sample	JAR-2A	JAR-2B	JAR-2C	JAR-2C	LU-5A	LU-5A	LU-5A	LU-5A	LU-5A	LU-5A	LU-5A	LU-5A	LU-5A	LU-5A
Point	an35	an12	an29	an35	an8	an11	an15	an16	an17	an18	an21	an28	an29	an45
SiO_2	0.04	0.00	0.01	0.02	0.01	0.03	0.00	0.02	0.02	0.04	0.02	0.02	0.04	0.03
TiO_2	0.11	0.00	0.02	0.05	0.00	0.02	0.13	0.06	0.18	0.08	0.01	0.04	0.02	0.08
Al_2O_3	22.31	24.43	26.87	24.91	24.92	9.48	23.77	27.69	21.15	14.79	14.86	25.36	21.19	27.11
Cr_2O_3	46.65	44.34	39.17	43.27	41.45	61.17	44.23	39.86	46.04	54.55	55.11	43.36	47.63	41.54
FeO	15.19	14.15	14.15	16.43	17.62	16.07	15.70	15.21	17.07	17.76	17.61	13.09	15.15	13.41
$Fe_2O_3^*$	1.49	0.80	3.16	1.49	2.96	0.19	1.59	1.68	2.30	0.00	0.00	1.27	1.43	0.79
MnO	0.24	0.22	0.24	0.27	0.31	0.28	0.28	0.20	0.26	0.29	0.29	0.18	0.23	0.21
MgO	12.84	13.47	13.54	12.23	11.36	10.79	12.46	13.18	11.35	9.84	10.23	14.31	12.69	14.19
NiO	0.08	0.06	0.13	0.06	0.09	0.08	0.13	0.13	0.10	0.05	0.07	0.13	0.08	0.11
ZnO	0.14	0.12	0.25	0.17	0.24	0.06	0.15	0.13	0.14	0.31	0.11	0.07	0.05	0.14
V_2O_5	0.19	0.15	0.13	0.18	0.13	0.24	0.24	0.21	0.23	0.22	0.26	0.20	0.22	0.24
Total	99.27	97.71	97.67	99.06	99.09	98.40	98.66	98.35	98.83	97.93	98.55	98.02	98.73	97.86
Formulae based on 3 cations. 4 O anions and iron valence calculation														
Si	0.00	0.00	0.00	0.00	0.00	0.00	0.00	0.00	0.00	0.00	0.00	0.00	0.00	0.00
Ti	0.00	0.00	0.00	0.00	0.00	0.00	0.00	0.00	0.00	0.00	0.00	0.00	0.00	0.00
Al	0.82	0.82	0.82	0.82	0.82	0.82	0.82	0.82	0.82	0.82	0.82	0.82	0.82	0.82
Cr	1.14	1.14	1.14	1.14	1.14	1.14	1.14	1.14	1.14	1.14	1.14	1.14	1.14	1.14
Fe^{3+*}	0.03	0.03	0.03	0.03	0.03	0.03	0.03	0.03	0.03	0.03	0.03	0.03	0.03	0.03
Fe^{2+}	0.39	0.39	0.39	0.39	0.39	0.39	0.39	0.39	0.39	0.39	0.39	0.39	0.39	0.39
Mn	0.01	0.01	0.01	0.01	0.01	0.01	0.01	0.01	0.01	0.01	0.01	0.01	0.01	0.01
Mg	0.59	0.59	0.59	0.59	0.59	0.59	0.59	0.59	0.59	0.59	0.59	0.59	0.59	0.59
Ni	0.00	0.00	0.00	0.00	0.00	0.00	0.00	0.00	0.00	0.00	0.00	0.00	0.00	0.00
Zn	0.00	0.00	0.00	0.00	0.00	0.00	0.00	0.00	0.00	0.00	0.00	0.00	0.00	0.00
V	0.00	0.00	0.00	0.00	0.00	0.00	0.00	0.00	0.00	0.00	0.00	0.00	0.00	0.00
Total	3.000	3.000	3.000	3.000	3.000	3.000	3.000	3.000	3.000	3.000	3.000	3.000	3.000	3.000
Cr#	0.58	0.55	0.49	0.54	0.53	0.81	0.56	0.49	0.59	0.71	0.71	0.53	0.60	0.51
Mg#	0.60	0.63	0.63	0.57	0.53	0.54	0.59	0.61	0.54	0.50	0.51	0.66	0.60	0.65
Fe^{2+}/Fe^{3+}	11.35	19.73	4.97	12.27	6.62	93.74	10.99	10.08	8.26	–	–	11.45	11.74	18.75
FeO/Fe_2O_3	10.21	17.75	4.47	11.04	5.96	84.35	9.89	9.07	7.43	–	–	10.30	10.56	16.87
*calculated														

Supplementary Table S3 – continuation

Locality	Ľutina	Ľutina	Ľutina	Ľutina	Ľutina	Ľutina	Ľutina	Ľutina	Ľutina	Ľutina	Ľutina	Ľutina
Formation	Malinowa Fm.	Malinowa Fm.	Malinowa Fm.	Malinowa Fm.	Malinowa Fm.	Malinowa Fm.	Malinowa Fm.	Malinowa Fm.	Malinowa Fm.	Malinowa Fm.	Malinowa Fm.	Malinowa Fm.
Age	Turonian–Campanian	Turonian–Campanian	Turonian–Campanian	Turonian–Campanian	Turonian–Campanian	Turonian–Campanian	Turonian–Campanian	Turonian–Campanian	Turonian–Campanian	Turonian–Campanian	Turonian–Campanian	Turonian–Campanian
Unit	Šariš U.	Šariš U.	Šariš U.	Šariš U.	Šariš U.	Šariš U.	Šariš U.	Šariš U.	Šariš U.	Šariš U.	Šariš U.	Šariš U.
Sample	LU-5A	LU-5A	LU-5A	LU-5A	LU-5A	LU-5B	LU-5B	LU-5B	LU-5B	LU-5B	LU-5B	LU-5B
Point	an46	an47	an48	an49	an50	an12	an18	an24	an25	an26	an27	an28
SiO_2	0.00	0.05	0.01	0.00	0.02	0.04	0.00	0.02	0.06	0.02	0.00	0.02
TiO_2	0.11	0.00	0.00	0.05	0.26	0.41	0.00	0.22	0.21	0.08	0.05	0.18
Al_2O_3	15.79	19.02	32.96	21.65	6.04	11.67	39.11	10.54	19.04	27.72	20.12	25.86
Cr_2O_3	49.20	48.50	35.27	47.35	60.85	56.05	27.34	57.71	45.07	40.56	47.52	42.88
FeO	19.80	17.45	12.56	14.29	21.87	14.83	12.85	20.28	17.68	12.91	16.83	12.53
$Fe_2O_3^*$	3.60	2.07	1.22	1.33	2.78	3.57	2.13	0.00	5.38	0.68	1.76	1.32
MnO	0.35	0.29	0.19	0.20	0.45	0.27	0.15	0.37	0.27	0.21	0.30	0.20
MgO	8.74	10.83	15.44	13.26	6.67	11.94	15.78	7.63	10.73	14.48	11.24	14.69
NiO	0.08	0.08	0.09	0.08	0.08	0.12	0.17	0.02	0.14	0.10	0.13	0.13
ZnO	0.27	0.19	0.11	0.05	0.13	0.04	0.17	0.23	0.06	0.04	0.19	0.15
V_2O_5	0.33	0.30	0.12	0.20	0.24	0.15	0.17	0.20	0.25	0.22	0.14	0.13
Total	98.27	98.77	97.97	98.47	99.39	99.08	97.86	97.24	98.88	97.01	98.27	98.10
Formulae based on 3 cations. 4 O anions and iron valence calculation												
Si	0.00	0.00	0.00	0.00	0.00	0.00	0.00	0.00	0.00	0.00	0.00	0.00
Ti	0.00	0.00	0.00	0.00	0.00	0.00	0.00	0.00	0.00	0.00	0.00	0.00
Al	0.82	0.82	0.82	0.82	0.82	0.82	0.82	0.82	0.82	0.82	0.82	0.82
Cr	1.14	1.14	1.14	1.14	1.14	1.14	1.14	1.14	1.14	1.14	1.14	1.14
Fe^{3+*}	0.03	0.03	0.03	0.03	0.03	0.03	0.03	0.03	0.03	0.03	0.03	0.03
Fe^{2+}	0.39	0.39	0.39	0.39	0.39	0.39	0.39	0.39	0.39	0.39	0.39	0.39
Mn	0.01	0.01	0.01	0.01	0.01	0.01	0.01	0.01	0.01	0.01	0.01	0.01
Mg	0.59	0.59	0.59	0.59	0.59	0.59	0.59	0.59	0.59	0.59	0.59	0.59
Ni	0.00	0.00	0.00	0.00	0.00	0.00	0.00	0.00	0.00	0.00	0.00	0.00
Zn	0.00	0.00	0.00	0.00	0.00	0.00	0.00	0.00	0.00	0.00	0.00	0.00
V	0.00	0.00	0.00	0.00	0.00	0.00	0.00	0.00	0.00	0.00	0.00	0.00
Total	3.000	3.000	3.000	3.000	3.000	3.000	3.000	3.000	3.000	3.000	3.000	3.000
Cr#	0.68	0.63	0.42	0.595	0.871	0.763	0.319	0.786	0.614	0.495	0.613	0.527
Mg#	0.44	0.53	0.69	0.62	0.35	0.59	0.69	0.40	0.52	0.67	0.54	0.68
Fe^{2+}/Fe^{3+}	6.11	9.38	11.44	11.98	8.75	4.61	6.70	–	3.65	21.09	10.63	10.55
FeO/Fe_2O_3	5.50	8.44	10.30	10.78	7.87	4.15	6.03	–	3.29	18.97	9.57	9.49
*calculated												

Supplementary Table S4

Representative microprobe analyses of pyroxene inclusions in detrital chromian spinels from Upper Cretaceous to Paleocene deposits of the Jarmuta-Proč Fm., structural drill JAR-2, Pieniny sector of the PKB, Western Carpathians, Slovakia

Locality	Ľutina	Ľutina	Ľutina
Formation	Malinowa Fm.	Malinowa Fm.	Malinowa Fm.
Age	Turonian–Campanian	Turonian–Campanian	Turonian–Campanian
Unit	Šariš U.	Šariš U.	Šariš U.
Sample	LU-5A	LU-5A	LU-5A
Point	an9	an10	an51
SiO_2	55.78	55.84	54.51
TiO_2	0.08	0.06	0.01
Al_2O_3	1.34	1.43	0.29
Cr_2O_3	0.92	0.95	1.64
Fe_2O_3	0.00	0.00	
FeO	5.12	5.46	1.68
MnO	0.14	0.15	0.04
MgO	34.51	34.49	17.67
CaO	0.44	0.39	24.32
Na_2O	0.00	0.00	0.23
Total	98.40	98.85	100.49
Formulae normalized to 6 oxygens.			
Si	1.95	1.94	1.98
Ti	0.00	0.00	0.00
Al	0.06	0.06	0.01
Cr	0.03	0.03	0.05
Fe^{3+}	0.02	0.02	0.00
Fe^{2+}	0.13	0.14	0.05
Mn	0.00	0.00	0.00
Mg	1.80	1.79	0.96
Ca	0.02	0.01	0.95
Na	0.00	0.00	0.00
Total	4	4	4.00
End members			
Wo	0.83	0.75	48.43
En	91.55	91.16	48.96
Fs	7.62	8.09	2.61